31 OCTOBER 1979 (FOUO 6/79) 1 OF 1

JPRS L/8742

31 October 1979

USSR Report

GEOPHYSICS, ASTRONOMY AND SPACE

(FOUO 6/79)

FBIS FOREIGN BROADCAST INFORMATION SERVICE

NOTE

JPRS publications contain information primarily from foreign newspapers, periodicals and books, but also from news agency transmissions and broadcasts. Materials from foreign-language sources are translated; those from English-language sources are transcribed or reprinted, with the original phrasing and other characteristics retained.

Headlines, editorial reports, and material enclosed in brackets [] are supplied by JPRS. Processing indicators such as [Text] or [Excerpt] in the first line of each item, or following the last line of a brief, indicate how the original information was processed. Where no processing indicator is given, the information was summarized or extracted.

Unfamiliar names rendered phonetically or transliterated are enclosed in parentheses. Words or names preceded by a question mark and enclosed in parentheses were not clear in the original but have been supplied as appropriate in context. Other unattributed parenthetical notes within the body of an item originate with the source. Times within items are as given by source.

The contents of this publication in no way represent the policies, views or attitudes of the U.S. Government.

For further information on report content call (703) 351-2938 (economic); 3468 (political, sociological, military); 2726 (life sciences); 2725 (physical sciences).

JPRS L/8742

31 October 1979

USSR REPORT

GEOPHYSICS, ASTRONOMY AND SPACE

(FOUO 6/79)

This serial publication contains articles, abstracts of articles and news items from USSR scientific and technical journals on the specific subjects reflected in the table of contents.

Photoduplications of foreign-language sources may be obtained from the Photoduplication Service, Library of Congress, Washington, D. C. 20540. Requests should provide adequate identification both as to the source and the individual article(s) desired.

CONTENTS PAGE

I. OCEANOGRAPHY

Translations UDC 551.462(267)

CONTINUOUS SEISMIC PROFILING IN THE OCEAN AT SPEEDS UP TO 15 KNOTS

Moscow OKEANOLOGIYA in Russian Vol 19, No 4, 1979 pp 718-724

[Article by Yu. P. Neprochnov, L. R. Merklin and I. N. Yel'nikov, Institute of Oceanology USSR Academy of Sciences, submitted for publication 18 October 1978]

Abstract: The authors examine the peculiarities of the method and the techniques for carrying out continuous seismic profiling when oceanographic vessels are proceeding at normal speed (13-15 knots). The article describes methods for towing pneumatic sound sources and detectors. The results of experimental investigations of the spectra and levels of recorded signals and noise are given. It is demonstrated that at speeds of 13-15 knots the developed method of continuous seismic profiling ensures a signal-to-noise ratio 15-20 db and penetration 2-3 km into the sedimentary strata in the ocean.

[Text] When carrying out a complex geophysical survey in the ocean while a ship is on course the only method restricting the speed of movement of ships to 8-10 knots is usually continuous seismic profiling. The main scientific research vessels of the Institute of Oceanology USSR Academy of Sciences have a high overall economical speed: "Vityaz'" -- 13 knots, "Akademik Kurchatov" and "Dmitriy Mendeleyev" -- about 15 knots. A decrease in the ship's speed for a long time is not always possible for technical and economic reasons and therefore on all geological-geophysical expeditions of the Institute of Oceanology on the large ships continuous seismic profiling has not been carried out along the entire track, but only on its individual segments, which has impaired the comprehensiveness of the geophysical survey. Similar difficulties can arise in geophysical work in the ocean by other organizations having high-speed vessels. Taking this circumstance into account, during recent years specialists at the Institute of Oceanology have developed a continuous seismic profiling method for a speed of 13-15 knots, which was successfully used on the 58th voyage of the scientific research vessel "Vityaz'" (1976) [5] and the 24th voyage of the scientific research ship "Akademik Kurchatov" (1977) [6].

General Characteristics of Continuous Seismic Profiling Method

In order to carry out the standard task of studying the structure of the sedimentary stratum and relief of the acoustic basement in the ocean in the process of an on-track complex geophysical survey the continuous seismic profiling (CSP) system usually consists of the following elements: 1) one or two sound sources, towed at a distance of 20-50 m from the vessel; 2) one or two pickup lines with a length of 30-50 m, towed on both sides of the ship at a distance of 200-300 m; 3) two recorders, making it possible to obtain time sections by the variable density method on electrochemical or electrothermal paper simultaneously at two paper speeds in different frequency ranges; 4) magnetic recorders, making possible subsequent reproduction of the records and processing of continuous seismic profiling data on an electronic computer for the purpose of increasing the resolution or effective depth of the investigations. On Soviet and foreign expeditions CSP is usually carried out at a ship speed up to 8-10 knots [4, 8, 10].

An increase in the speeds of movement of a ship to 15 knots during CSP involves certain technical and methodological difficulties. With an increase in the ship's speed there is a decrease in the depth of submergence of the sound sources and detectors until they pop out on the surface; there is a marked increase in the level of the registered noise due to an increase in vibration of the towing cable and receiving section, and also the turbulence of the water boundary layer on the surface of the hose covering the pickup line [2, 10]. In addition, at speeds of about 15 knots the detonation interval attains 70-100 m, exceeding by a factor of 2-3 the length of the standard receiving lines. A solution for the enumerated problems was brought about in three ways: 1) by the use of heavy designs of the pneumatic sound sources with increased power with improved hydrodynamic streamlining characteristics, 2) improvements in the schemes for towing the sound sources and detectors, 3) use of noise-immune designs of a receiving section of increased length.

Pneumatic Sound Sources

For towing at maximum speeds use was made of pneumatic sound sources of the "Impul's-1" type (designed by the "YuZhMORGEO" scientific and production combine) in two variants: with a volume of the high-pressure chamber 3 liters and 2 x 3 liters weighing 70 and 140 kg respectively. The paired sound source consisted of two chambers, each with a volume of 3 liters, joined into a group and opening from one electromagnetic valve synchronously or with a lag relative to one another. The following scheme (Fig. 1,a) was tested for deepening the sound sources: the pneumatic sound source was towed on a cable with a length of 100-120 m, the attachment of the tow line was on the prow of the vessel near the waterline; lowering and raising operations were carried out from the ship's stern. Using this scheme a pneumatic sound source 2 x 3 liters was towed at a depth of 5-7 m with a ship's speed of 15 knots. For this same deepening the lighter chamber with a volume of 3 liters a tear-shaped static weight (50 kg) was incorporated in the towing line. An increase in the speed of towing to 15 knots also caused an increase in the mechanical loads on the air line due to its high drag in the case of noncoaxial flow around the object. Therefore, as the electric cable use was made of a KPMM cable with a breaking strength 700 kg, to which an air line was attached. This made it possible to use it as a load-carrying cable. The attachment of the high-pressure line to it was accomplished in such a way that the air hose could move freely in a longitudinal direction relative to the cable at the points of attachment, not allowing the formation of loops and thereby eliminating bending moments on the cable strands.

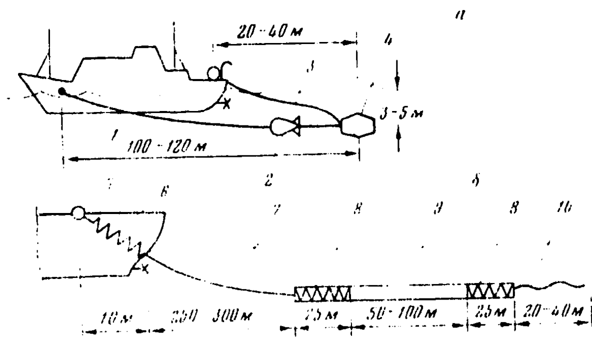

Fig. 1. Scheme for the towing of pneumatic sound sources (a) and detectors (b). 1) towing cable; 2) tear-shaped static weight; 3) high-pressure air line; 4) sound source; 5) on-board crane; 6) rubber shock absorber; 7) towing cable; 8) shock-absorber sections; 9) working section with piezodetectors; 10) trailing line

The amplitude-frequency characteristics of the "Impul's-1" pneumatic sound sources (Fig. 2) show that for the working depths of submergence in the region of the low frequencies the signal level is decreased with a decrease in depth. However, in the frequency band 40-80 Hz the intensity of radiation for different depths is approximately identical, which makes it possible to use filtering of the receiving-recording apparatus in the frequency range most favorable with respect to receiver noise (Fig. 3). The method for towing the pneumatic sound source indicated a high reliability, ensuring the carrying out of continuous observations over a long period of time without failures; the maximum duration of continuous operation of a single sound source was 132 hours (5.5 days). During towing of pneumatic sound sources on the two sides of the ship the duration of CSP was virtually unlimited due to the alternate operation of the sound sources.

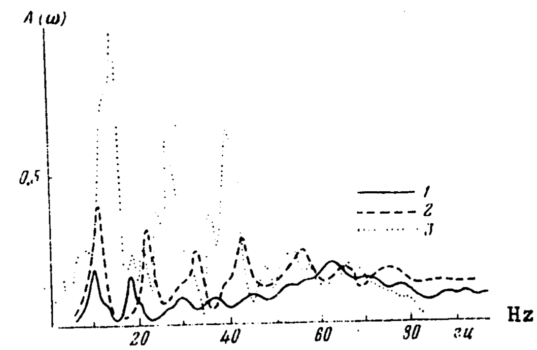

Fig. 2. Amplitude spectra of sounding pulse emitted by pneumatic chamber of "Impul's-1" apparatus with a volume of 3 liters at depths of 3 (1), 5 (2) and 10 m (3).

Detectors

During CSP at a speed of 15 knots the receiving apparatus was towed on a special cable of the KPMM type with a length up to 300 m, ensuring a depth of submergence of the receiving apparatus to 7-10 m, which is the limit for such speeds, the diameter and weight of the towing cable and the dimensions of the receiving section. An increase in the noise immunity of the reception was attained by an improvement in the scheme for towing of the apparatus and construction of the receiving channel. The towing of the receiving apparatus (Fig. 1,b) was accomplished by means of a special boom ensuring shifting of the towing point 8-10 m to one side of the ship for getting away from the most disturbed part of the wake.

The towing cable is attached to the boom by means of a 3-4-link rubber shock absorber with a length of 10-12 m, selected experimentally.

Vacuum rubber proved to be the most successful material for the shock absorbers. Each link of the shock absorber with a length of 3-4 m is assembled from several segments of a cord of vacuum rubber with a diameter of 15-30 mm in such a way that with a stipulated rate of towing the link was drawn out no more than 30% of its length and with a further increase in speed the towing load was imparted to a Kapron safety line. Good results with the suppression of jerks and vibrations of the towing ship were demonstrated by three-link shock absorbers with successive arrangement of the links, rated for 8, 12 and 15 knots.

On both sides of the hose receiving section with a length of 50-100 m there are also hose sections without instruments, each with a length of 10-25 m, intended for additional mechanical and acoustic "decoupling" of the receiving section from the towing cable and the trailing line. The trailing line with a length of 20-30 m ensures stabilization of motion of the receiving section in the water and the absorption of low-frequency vibration of wave interference [1, 2]. The boom is installed in the midships region. This results in a minimum yawing of the receiving apparatus on course and precludes the influence of keel rolling, whereas a decrease in side-to-side rolling is ensured by special dampers such as exist on ships of the "Akademik Kurchatov" type.

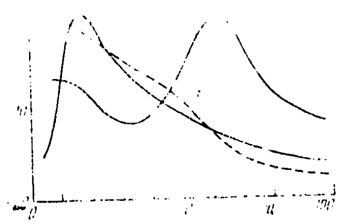

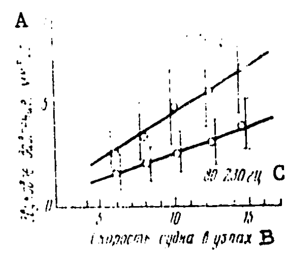

Fig. 3. Envelopes of normalized amplitude spectra of signals of pneumatic sound source and noise of towed receiving apparatus. 1) spectrum of signal of pneumatic sound source towed at depth of 10 m; 2) same at depth of 3 m; 3) noise spectrum of receiving apparatus at speed of 15 knots.

Fig. 4. Dependence of levels of recorded noise on speed of towing in different frequency ranges of recording (the vertical lines show the range of fluctuation of noise levels). A) Sound pressure, μbar; B) Ship speed in knots; C) Hz

The design of the receiving section is traditional: within an oil-filled PVKh-hose with a diameter of 44 mm there is a group of piezodetectors resistant to vibrations and a preamplifier. The number of piezodetectors and the scheme for their grouping are selected in dependence on the work method, the speed of towing, the type of sound source and the required range of recording frequencies. For high towing speeds (10-15 knots) and the low-frequency range (10-100 Hz) the most effective grouping schemes are those with a triangular envelope of the distribution of response and optimization of the grouping interval for the piezodetectors [3], for example, a group of 42 or 64 PDS-7 piezodetectors on a base of 44 and 70 m respectively. An important peculiarity of the design of the receiving section is the absence of a load-bearing cable, whose functions are performed by the hose covering the section, thereby reducing the direct transfer of vibrations of the receiving apparatus to the piezodetector. In this case the length of the strand of wires within the section, to which the piezodetectors are attached, must be not less than 15% longer than the outer hose so that with a maximum speed of towing, and accordingly, a maximum lengthening of the hose, the towing force is not imparted to the wires with the piezodetectors.

Special measurements on the 24th voyage of the scientific research ship "Akademik Kurchatov" indicated that the described towing system and the design of the receiving apparatus, at a speed of 15 knots, ensure a noise level at the receiving channel output of 3-4 μbar in the frequency band 80-230 Hz (0.03 μbar/Hz) and 6-7 μbar in the band 20-75 Hz (0.15 μ bar/Hz) with a characteristic linear dependence of the noise levels on the speed of towing (Fig. 4).

Some Results

The developed method and apparatus for CSP at ship speeds up to 15 knots make it possible to obtain a signal-to-noise ratio of 15-20 db (Fig. 5), making it possible to trace both the reflecting discontinuities within the sedimentary stratum and the surface of the acoustic basement in the ocean. In the course of the 58th voyage of the scientific research vessel "Vityaz'" and the 24th voyage of the scientific research vessel "Akademik Kurchatov" by use of such a method it was possible to carry out more than 31,000 km of CSP profiles with an effective depth of investigations in the sedimentary stratum up to 2-3 km in dependence on seismological conditions. Figure 6 shows examples of CSP records obtained at speeds of 13 knots in the Indian Ocean and 15 knots in the Atlantic Ocean.

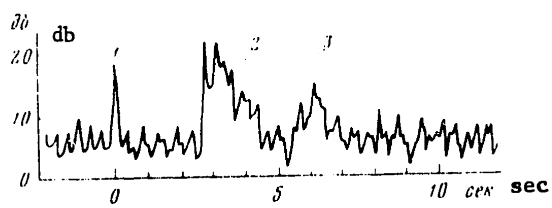

Fig. 5. Example of record of signal and noise levels of one seismic trace with ship speed 15 knots. 1) direct wave; 2) reflections from bottom and boundaries beneath bottom; 3) second full reflections.

In the axial part of the Sonda abyssal trench (ocean depth 6.0-6.3 km), filled with well-stratified sediments with a thickness up to 1.5 km, it is easy to discriminate the dislocated surface of the acoustic (basalt) basement Ф, plunging beneath the island slope (Fig. 6,a). The dislocations associated with the boundaries of small basement blocks are traced through the entire sedimentary stratum and are expressed in the bottom relief in the form of small projections with an amplitude of 20-50 m.

On the CSP profile in the Canaries basin of the Atlantic Ocean near the Cape Verde Islands (ocean depth about 4 km) a study was made of a sedimentary stratum with a thickness of 1-3 km, covering the highly dissected surface of the basement Ф (Fig. 6,b). In the sedimentary stratum at a depth of about 250 m it is easy to trace the reflecting boundary A, corresponding to the known Eocene unconformity in the North Atlantic [9], and at a depth of about 1 km beneath the bottom -- the reflecting boundary β, correlating, according to deep drilling data, with the boundary between the layer of black clays and Lower Cretaceous limestones underlaying them [7, 11].

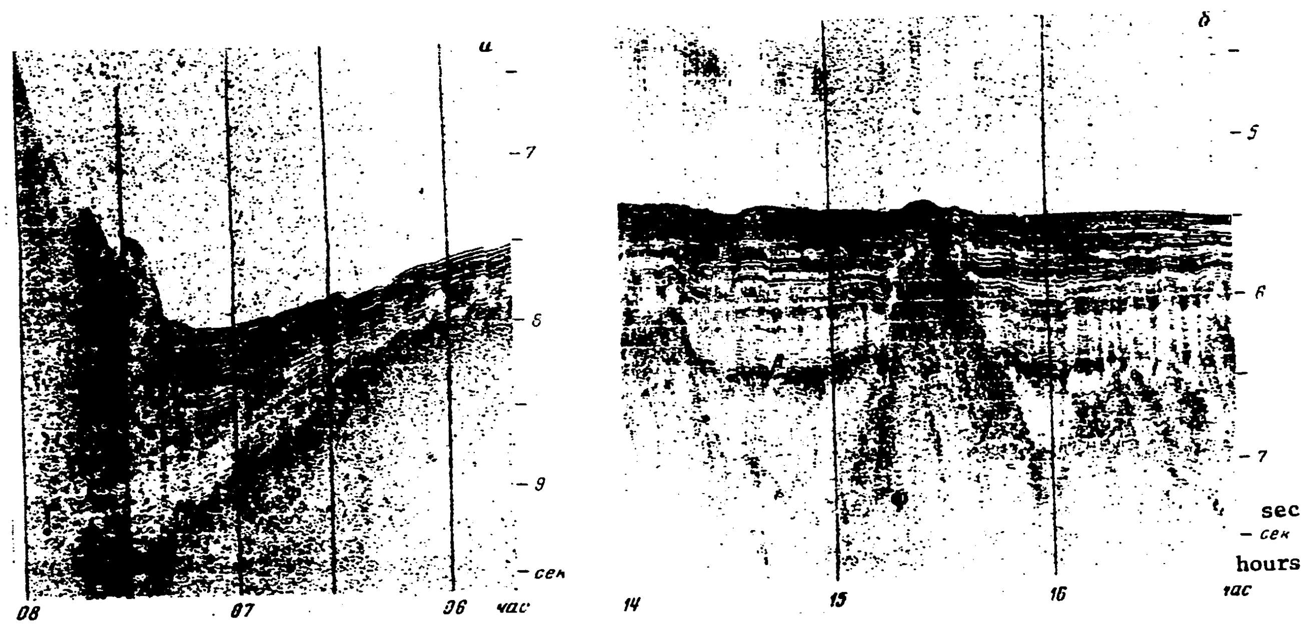

Fig. 6. Examples of continuous seismic profiling records. a) speed of 13 knots, pneumatic sound source with volume of 3 liters (58th voyage of the scientific research vessel "Vityaz'" in Sonda trench in Indian Ocean); b) speed of 15 knots, pneumatic sound source with volume of 6 liters (24th voyage of the scientific research vessel "Akademik Kurchatov," Canaries basin, Atlantic Ocean).

Experience in various types of seismogeological conditions (ridges, ocean basins, abyssal trenches) demonstrated that the developed method and equipment for CSP at speeds of 13-15 knots makes possible a reliable study of the structure of the sedimentary stratum and relief of the acoustic basement in the ocean. The use of this method will broaden the possibilities for carrying out a comprehensive geophysical survey in the oceans on all the tracks of oceanographic vessels.

BIBLIOGRAPHY

1. Lunarskiy, G. N., "String of Piezodetectors for Seismic Profiling," Deposited at the All-Union Institute of Scientific and Technical Information, No 832-75, 1975.

2. Merklin, L. R., Gagel'gants, A. A., Podshuveyt, V. B., Turapina, A. N., Shishanov, G. V., "Receiving Devices and Some Types of Interference in Sea Seismic Prospecting (Review)," MORSKAYA GEOLOGIYA I GEOFIZIKA (Marine Geology and Geophysics), Moscow, VIEMS, 1973.

3. Merklin, L. R., Sheremet, I. A., "Optimization of Complex Discrete Interference Systems in Sea Seismic Prospecting," VOPROSY DINAMICHESKOY TEORII RASPROSTRANENIYA SEYSMICHESKIKH VOLN (Problems in the Dynamic Theory of Seismic Wave Propagation), 12, Moscow, "Nauka," 1974.

5. METODIKA GEOFIZICHESKIKH ISSLEDOVANIY OKEANOV (Methods for Geophysical Investigations of the Oceans), edited by S. M. Zverev, Moscow, "Nauka," 1974.

5. Neprochnov, Yu. P., "Fifty-Eighth Voyage of the Scientific Research Vessel 'Vityaz''," PRIRODA (Nature), No 11, 1976.

6. Neprochnov, Yu. P., "Twenty-Fourth Voyage of the Scientific Research Vessel 'Akademik Kurchatov'," OKEANOLOGIYA, Vol 18, No 1, 1978.

7. Edgar, N.T., "Acoustic Stratigraphy in the Deep Oceans," THE GEOLOGY OF CONTINENTAL MARGINS, Springer-Verlag, N. Y., 1974.

8. Freitag, J. S., Holcombe, T. L., Pew, J. A., "Oceanographic and Data Processing Instrumentation Aboard USNS Kane for Cruise Nine," UNDERSEA TECHNOLOGY HANDBOOK DIRECTORY, Ch 5, A/31-A/44, 1969.

9. Hayes, D. E., Pimm, A. C., et al., INITIAL REPORTS OF THE DEEP SEA DRILLING PROJECT, XIV, US Print Office, Washington, 1972.

10. Knott, S. T., Bunce, E. T., "Recent Improvements in Technique of Continuous Seismic Profiling," DEEP SEA RES., 15, 1968.

11. Peterson, M. N. A., Edgar, N. T., Von der Borch, C., et al., INITIAL REPORTS OF THE DEEP SEA DRILLING PROJECT, II, US Print Office, Washington, 1970.

[8144/0056-5303]

5303
CSO: 8144 /56

UDC 550.834(261.24)

EXPERIENCE IN CARRYING OUT SEISMIC OBSERVATIONS BY THE REFRACTED WAVES METHOD IN THE BALTIC SEA

Moscow OKEANOLOGIYA in Russian Vol 19, No 4, 1979 pp 712-717

[Article by A. A. Geodekyan, Yu. P. Neprochnov, I. N. Yel'nikov, I. T. Dubovskoy, A. A. Pokryshkin, Yu. D. Yevsyukov and N. I. Sviridov, Institute of Oceanology, submitted for publication 21 March 1977]

Abstract: The paper presents the results of experimental-methodological work by the refracted waves method along three profiles on the 16th expedition of the scientific research ship "Akademik Kurchatov" in hypothetically petroleum- and gas-bearing parts of the Baltic syneclise (Baltic Sea). The objective of the work was a clarification of the possibilities of this method for detecting deep-lying discontinuities of the sedimentary mantle and the crystalline basement under conditions of extremely shallow water bodies. The source of the elastic oscillations was a pneumatic sound source; the recorders were bottom seismographs. It is shown that there is an essential possibility for employing the refracted waves method in its modern instrumental form in shallow-water areas. The prospects for increasing the "effective depth" of the method involve an optimization of the method for placement of bottom seismographs and an increase in the volume of the pneumatic chambers for the sources of elastic oscillations.

[Text] On the 16th specialized voyage of the "Akademik Kurchatov" (October 1973), in the cycle of investigations directed to study of the possibilities of finding petroleum and gas in the sea portion of the Baltic syneclise of the East European Platform, experimental-methodological work was carried out by the refracted waves method [1]. The purpose of the work was clarification of the possibility of employing this method in its modern instrumental design for the detection of deep-lying discontinuities in the possibly petroleum- and gas-bearing sedimentary mantle and within its crystalline basement under the conditions prevailing in shallow seas. As the source of elastic oscillations use was made of a pneumatic sound source; the recorders were bottom seismographs.

The pneumatic sound source in studies by the refracted waves method at sea came into use relatively recently -- in 1971 [2]. It consists of a group of four chambers of the design produced by the Ramenskoye Division of the All-Union Scientific Research Institute of Geophysics. The volume of each chamber is 7 liters. On the preceding expeditions of the Institute of Oceanology USSR Academy of Sciences such a sound source was used in the Black Sea and in the Indian Ocean -- in abyssal regions with a thick sedimentary cover. The use of bottom seismographs as recorders in shallow-water seas ($<$ 1000 m) was problematical [4]. It is known that the level of seismic noise in the range 2-15 Hz at the sea floor, beginning with a depth of 1000-1500 m and below, corresponds to its mean level on the continent. In extremely shallow-water basins of the Baltic Sea type (at depths 50-200 m) the level of low-frequency microseisms can be still greater. For this reason bottom seismographs usually have not been used in such seas.

In the considered region (Fig. 1) observations by the refracted waves method were carried out earlier by American researchers [5]. The work was carried out using two ships; the sources of elastic waves were detonations of TNT charges. As a result, refracted waves were obtained from the surface of the crystalline basement and two above-lying discontinuities in the sedimentary layer. The depth of the crystalline basement (refracting discontinuity with a velocity 5.6-6.0 km/sec) was equal to 1.5-2.5 km. According to data from continuous seismic profiling [1], the layer of unlithified sediments has a small thickness (30-70 m) in the sea. The remaining part of the ancient platform cover to the basement surface was represented by deposits of the Cenozoic, Mesozoic and hypothetically petroleum-bearing rocks of the Paleozoic.

The pneumatic source, with the discharge of air compressed to 100 atm, excites elastic oscillations in a relatively narrow frequency spectrum -- 10-25 Hz (in dependence on the depth of submergence of the source chamber beneath the water surface). Therefore, the carrying out of seismic observations in the Baltic by the refracted waves method with such a source is interesting in order to detect in a shallow sea the "useful signal-noise" relationship.

Thus, the region of experimental-methodological investigations is extremely attractive in both practical and methodological respects.

Experimental method. In the processing of each seismic profile the bottom seismograph was placed in its central part. Then the vessel moved along with a speed of 5 knots toward one of the ends of the profile and passed it, towing the pneumatic source. Such a relatively simple method ensured obtaining travel-time curves of the refracted waves, making it possible to determine the boundary velocities of layers in the earth's crust.

The method for placement of the bottom seismograph differed from that usually employed in abyssal regions when the instrument is lowered to the bottom under the influence of its own weight [3]. In a shallow sea there is no parachuting effect during the falling of the instrument due to tugging on the Kapron cable and foam plastic buoy and therefore the bottom seismograph, dropping down into the water, develops a great velocity. Upon impact on the bottom, individual working units of the instrument can be put out of operation due to mechanical damage. Therefore, when placing the seismograph the first component to be lowered is the capsule with the instrument, then the anchor weight, and last the floating marking buoy.

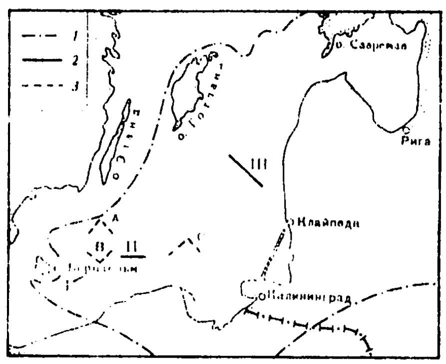

Fig. 1. Layout of refracted waves method seismic profiles in sea portion of syneclise (Baltic Sea). 1) contours of Baltic syneclise; 2) profiles run by an expedition of the scientific research vessel "Akademik Kurchatov"; 3) profiles run by American researchers [5].

The seismograph capsule withstands a water pressure corresponding to a basin depth of 5 km, but the sea floor depths at the points of placement of the bottom seismographs in the Baltic was only about 100 m. The capsule was joined by a Kapron cable 10-12 mm in diameter to an anchor weight weighing 70 kg and a foam plastic marking buoy. The length of the cable between the anchor weight and the instrument was 50-60 m.

The placement of a bottom seismograph in shallow waters requires excellent organization and working skills. It is necessary to place the instrument on the bottom in such a way that the cable between it and the anchor weight is not taut. Otherwise all the "tugs" from the floating marking buoy would a

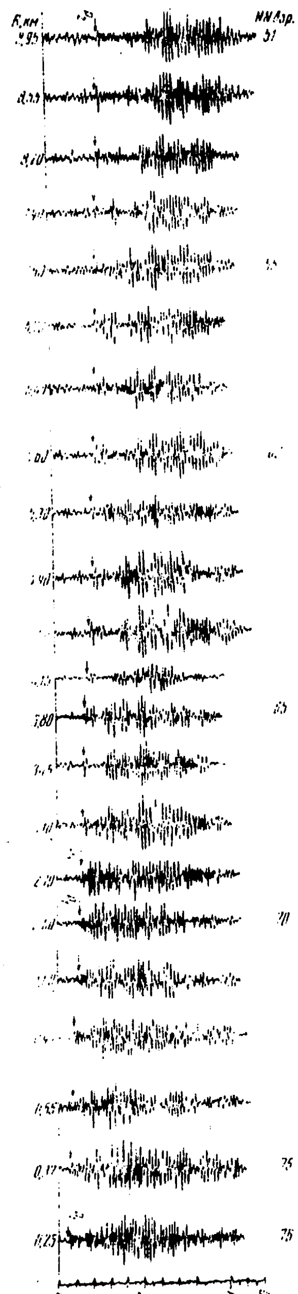

b

Fig. 2. Example of seismic record along profile III. a) number of shot point; b) sec

be transmitted through the weight to the instrument. With waves at sea above class 3 and with drifting of the vessel at a speed greater than 1 knot it was not possible to free the instrument from the "tugs" of the freely floating buoy. The length of the Kapron cable between the marking buoy and the anchor weight exceeded the sea depth at the point where the bottom seismograph was placed by some additional value which was usually 50-60% of the depth. Such a regulation of cable length ensured freeing of the instrument from the tugs of the floating marking buoy.

The pneumatic source was towed behind the vessel at a depth of 20 m from the water surface. The compressed air was released each 0.5-2 minutes. Thus, with a ship's speed of about 5 knots the intervals between the impulses of radiation of elastic oscillations was only 75-300 m. Such a density of observation points corresponds to the detail of investigations by the deep seismic sounding method on land. The carrying out of such detailed observations on the voyage was possible due to the presence of a high-pressure compressor aboard the vessel with a productivity of compressed air of about 33 liters/minute with its pressure up to 100 atm.

The moments of radiations of elastic oscillations were registered by a H327-5 automatic recorder using a hydrophone consisting of five crystals of PKS-4 piezoceramic and a matching transformer. The automatic recorder was also fed time marks from an on-board quartz clock with a coded signal which recorded the day, hour and minute of the radiation time. The bottom seismographs used ordinary 6-MKh sea chronometers.

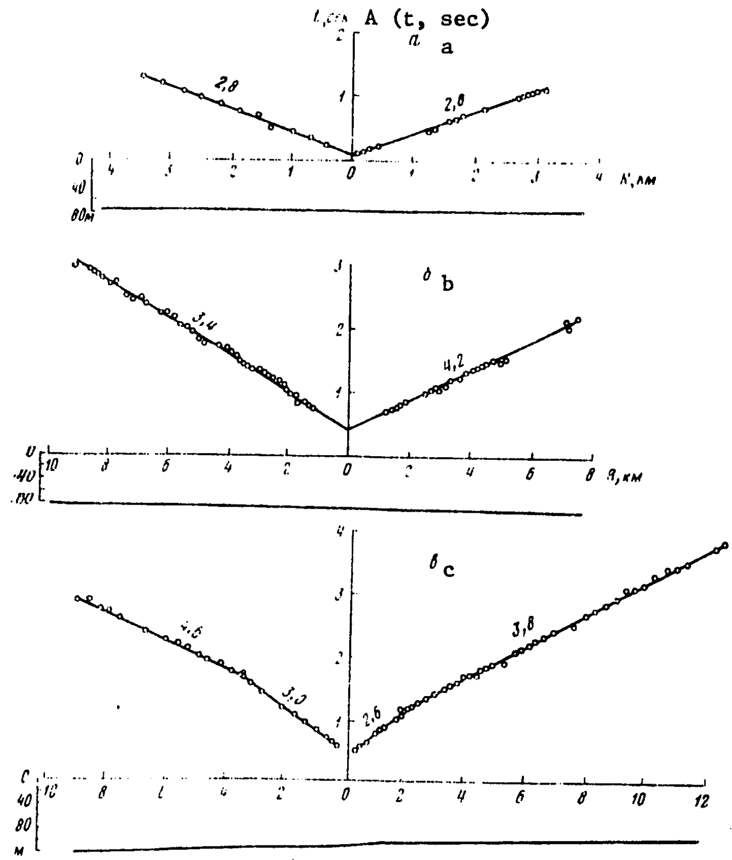

Fig. 3. Travel-time curves of refracted waves and sea bottom relief along profiles I (a), II (b), III (c). A) sec

On the voyage use was made of single-component seismographs with LF amplifiers of the balance type whose amplification factor was 2,000-7,000. The current supply for the entire bottom seismograph (BS) system was from galvanic cells of the "Mars" type.

The length of each of the refracted waves method profiles worked on the voyage was 20-35 miles. These profiles were run when waves were not more than class 3.

Research results. The observations were made along six profiles, but only along three of them was it possible to avoid "tugs" of the marking buoy and discriminate useful signals (Fig. 2).

The level of seismic noise on the bottom seismograph records, obtained on the voyage, exceeds that for abyssal seas by a factor of 3-4. For example, whereas in the abyssal part of the Black Sea (depth greater than 1.5 km) on the floor it was possible to register useful signals of 2-3 μV, in the waters of the Baltic the useful signals are registered beginning only with 8-10 μV and above.

At points where the bottom seismographs were set out determinations were made of the temperature and salinity of sea water at different bathymetric horizons. Using these data it was possible to compute the velocity values for the propagation of sound in the water and graphs of its dependence on depth were constructed. As a result, it was possible to determine the mean vertical speed of sound in water, which for all profiles was found to be 1450±5 m/sec. This velocity was used in computations in the interpretation of travel-time curves.

All attempts to discriminate a direct sound wave on the records were unsuccessful. Therefore, the position of the bottom seismograph and the points of radiation of elastic waves on the profiles were determined using only data from the radionavigation satellite system of the ship.

Profile I (Figures 1 and 3), with a length of 25 km, was situated on the southeastern periclinal structure of the Bornholm rise, in the zone of presence of rocks of the Silurian beneath the unconsolidated Quaternary deposits, and is oriented in a sublatitudinal direction. After placement the bottom seismograph temporarily malfunctioned due to impairments in the electronic circuitry of the amplifier. For this reason the record with registry of refracted waves was obtained only for the western part of the profile. Along the profile, at a distance 0.1-3.5 km from the bottom seismograph, it was possible to trace refracted waves from the bottom surface with a boundary velocity 2.8 km/sec (Fig. 3). The data from work carried out on the voyage by the CSP method and by dredging indicate that in this region the bottom surface consists of Silurian deposits with a virtual absence of a cover of unconsolidated sediments.

Profile II, run 60 km to the east of profile I, has a latitudinal orientation. At a distance of 20 km to the west is profile B, run by American researchers (Fig. 1), along which there was registry of refracted waves with velocities of 1.79 km/sec (second arrivals), 3.2-3.7 km/sec (first arrivals) -- at a distance from the registry points 0.1-1.8 km; 4.8-4.9 km/sec (first arrivals) at a distance 1.8-9.0 km; 6.0 km/sec (first arrivals) -- farther along the profile. On our profile in the first arrivals we registered a wave with an apparent velocity 3.4-4.2 km/sec. It is traced in the range of distances from the bottom seismograph 1.2-10 km (Fig. 3) and then attenuates. Thus, the refracting boundary has a slope from east to west; its boundary velocity is 3.8 km/sec and the depth of this boundary at the site of placement of the bottom seismograph is 300 m from the bottom surface (with an arbitrarily assumed velocity in the bottom deposits of 2.0 km/sec). Judging from these data, and also taking into account the results of CSP and dredging [1], it can be assumed that this boundary corresponds to the top of the Ordovician rocks, represented by the calcareous facies.

At a number of points on the profile it is also possible to discriminate an intensive wave with an apparent velocity 1.45 km/sec, but this is not a direct sound wave because its travel-time curve is 0.3 sec above the computed value.

Profile III, with a NW orientation, is situated in the region of a major brachyanticlinal rise in the Liyepaya Sea (Figures 1, 2 and 3). In the first arrivals along the profile there is registry of two refracted waves: the first in the range of distances from the bottom seismograph 0.1-3.4 km with a velocity 2.8 km/sec; the second in the range 2-12.2 km, is characterized by a boundary velocity 4.2 km/sec. The refracting boundaries plunge in a direction from NW to SE; their depth at the point of instrument placement is 370 and 830 m respectively from the bottom surface. On this basis, and with CSP materials taken into account, the first of them can be identified with the top pf the Silurian, and the second with the top of Ordovician deposits. The irregular waves which are discriminated against the noise background are tracked along the profile for a distance up to 21 km from the bottom seismograph.

Conclusions

On the basis of our experimental-methodological work it was possible to ascertain a fundamental possibility for using bottom seismographs under the conditions prevailing in a shallow sea as the recording points in observations by the refracted waves method with the use of pneumatic sound sources. In such work particular attention must be given to the choice of a rational method for the placement of bottom seismographs for the purpose of "decoupling" of instruments from sea surface waves.

The use of a pneumatic sound source, consisting of four chambers with a total volume of 28 liters, did not make it possible, in the Baltic Sea, to study refracting boundaries with velocities exceeding 4.2 km/sec. This, evidently, is associated with the absence of low-frequency components (below 10 Hz) in the radiation spectrum. When carrying out investigations by the refracted waves method in shallow waters in order to detect deep-lying refracting discontinuities with high boundary velocities it is necessary to use large-volume chambers as the pneumatic sources of elastic oscillations.

BIBLIOGRAPHY

1. Geodekyan, A. A., "Preliminary Scientific Results of Geological-Geophysical and Geochemical Expeditionary Work on the 16th Voyage of the Scientific Research Vessel 'Akademik Kurchatov' in the Baltic Sea," OKEANOLOGIYA (Oceanology), Vol 14, No 4, 1974.

2. Neprochnov, Yu. P., Yel'nikov, I. N., Kholopov, B. V., Semenov, G. A., Moskalenko, V. N., Yevsyukov, Yu. D., "Deep Seismic Sounding in the Ocean With Use of Pneumatic Sources of Elastic Waves," OKEANOLOGIYA, Vol 14, No 1, 1974.

3. Rykunov, L. N., Sedov, V. V., "Seismic Noise in the Frequency Range 2-15 Hz on the Floor of the Black Sea," IZV. AN SSSR, FIZIKA ZEMLI (News of the USSR Academy of Sciences, Physics of the Earth), No 7, 1965.

4. Rykunov, L. N., Sedov, V. V., "Bottom Seismograph," IZV. AN SSSR, FIZIKA ZEMLI, No 8, 1967.

5. Bunce, T., "Seismic Refraction Measurements in the Baltic Sea," GEOPHYS. PROSPECT., 17, No 1, 1969.

[8144/0057-5303]

5303
CSO: 8144/57

II. UPPER ATMOSPHERE AND SPACE RESEARCH

Translations

EFFECTS IN COSMIC RAYS ON 4-5 AUGUST 1972 ACCORDING TO MEASUREMENTS MADE ABOARD THE 'PROGNOZ-2' STATION

Moscow PROBLEMY SOLNECHNOY AKTIVNOSTI I KOSMICHESKAYA SISTEMA "PROGNOZ" in Russian 1977 pp 136-143

[Article by N. N. Volodichev, N. L. Grigorov, G. Ya. Kolesov, Ye. I. Morozova, A. N. Podorol'skiy, I. A. Savenko and A. A. Suslov]

[Text] During the period 2-9 August 1972 there were considerable and unusual changes in the intensity of cosmic rays associated with the activity of the active region Mc Math 11976 on the sun. Interest in these events is great, but due to the complexity of the transpiring phenomena more or less fundamental studies of cosmic rays with model representations have only recently begun to appear for the mentioned period [1, 2].

However, it is noted in these studies that the represented models are qualitative, and for the invocation of rigorous theoretical models it is necessary to have more detailed experimental data.

This paper gives some experimental results obtained on the "Prognoz" stations for the period 4-7 August 1972.

Forbush Effect in Proton and Nuclear Components

The first Forbush effect in cosmic rays began on 4 August at 0200 UT. Its onset can be seen clearly for protons ($E_p \geqslant 500$ MeV) and nuclei with $Z \geqslant 6$ ($E_{kin} \geqslant 600$ MeV/nucleon) on the basis of data from measurements on the "Prognoz-2" station and for the neutron component of secondary cosmic rays on the basis of neutron monitor data (Fig. 1).

On 4 August ground stations registered two sudden commencements of a magnetic storm (SC) at 0119 and 0220 UT from chromospheric flares on the sun on 2 August (the vertical dashed lines in Fig. 1).

At about 0700 UT, when the amplitude of the decrease in the proton component of cosmic rays was $\sim 10\%$ (in the neutron component $\sim 6\%$), there was onset of a rapid increase in the counting rate of protons with $E_{kin} \geqslant 500$ MeV, associated [3] with the generation of cosmic rays in a solar flare of importance 3B, whose maximum phase was observed [4] at 0640 UT. The decrease in the intensity of nuclei of galactic cosmic rays (GCR) with $Z \geqslant 6$ continued. It could be traced to 1100 UT, after which the "Prognoz-2" station entered the near-earth segment of the trajectory (from 1100 to 1300 UT). At 1100 UT the amplitude of the decrease for GCR nuclei with $Z \geqslant 6$ was 30±9%, in the neutron component 7-8% according to data from high-latitude neutron monitors [1]. Between 1300 and 2300 UT there was a small (~30%) increase in the flux of nuclei with a charge $Z \geqslant 6$, evidently of galactic origin.

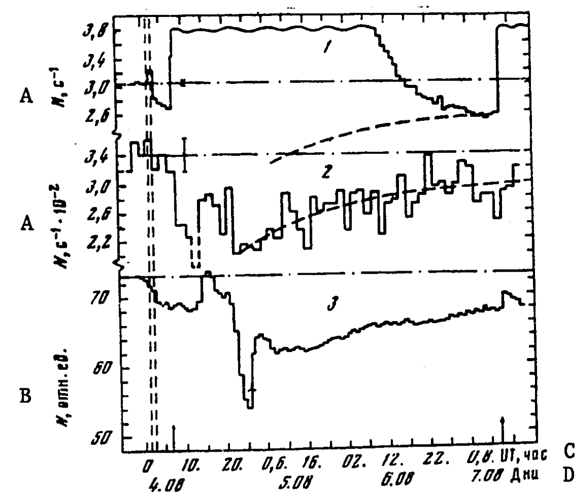

Fig. 1. Solar cosmic rays (SCR) and Forbush effect in proton and nuclear components of cosmic rays 4-7 August 1972. 1) counting rate of protons ($E_{kin} \geqslant 500$ MeV); 2) counting rate of nuclei with charge $Z \geqslant 6$ ($E_{kin} \geqslant 600$ MeV/nucleon); 3) readings of neutron monitor (Apatity); arrows -- solar chromospheric flares; dashed lines (curves) -- averaged profile for nuclei with $Z \geqslant 6$.

KEY:

A. sec
B. relative units
C. hours
D. days

At 2054 UT on 4 August the ground stations registered a new SC from a flare of importance 3B at 0621 UT on 4 August, after which a second Forbush effect began in the cosmic rays. In the nuclear component of the GCR the amplitude of the decrease at the minimum of the Forbush effect for nuclei with $Z \geqslant 6$ was ~ 40±9%; for high-latitude neutron monitors the degree of the decrease was $\sim 25\%$ [1]. (The amplitudes of the decreases are reckoned from the mean values for the "quiet" period 1-3 August 1972 and are represented in Fig. 1 by the horizontal dot-dash lines.) We note that from a comparison of the amplitudes of the intensity decreases in GCR in accordance with the data from the "Prognoz-2" station for nuclei with $E_{kin} \geqslant 600$ MeV/nucleon and for high-latitude neutron monitors it follows that the ratio of these amplitudes for the second Forbush effect is a value 1.4±0.2; such a relationship does not agree with the value of the spectral exponent of the Forbush effect $\gamma =$ 1.2, obtained in [1]. In actuality, in a number of experiments with balloons [5] and satellites [6] for the spectrum of the Forbush effect in the form $\delta D/D \sim \varepsilon^{-\gamma}$, where $\gamma = 0.8$, the corresponding ratio of the decrease amplitudes is $\approx$ 3-4. We note that for the first Forbush effect the corresponding ratio is $\sim$ 3-4.

An investigation of the temporal dependence of the intensity of protons and nuclei of GCR in the restoration phase of the second Forbush effect indicated that this phase for protons and nuclei with $Z \geqslant 2$ and $Z \geqslant 6$ transpires identically (the ratio of the amplitudes of the decreases is identical). A similar conclusion with an accuracy to $\sim 4\%$ can also be drawn for nuclei with $Z \geqslant 15$ with the averaging of data for Δt = 3 days (such a time interval is still reasonable because the restoration phase is $\geqslant 10$ days).

Solar Cosmic Rays from Flare of 4 August 1972

The initial phase of the increase in the intensity of SCR from the flare of 4 August has been described in [3]. The intensity maximum for SCR from this flare was attained for energies of about several tens of MeV (data from the satellites IMP-5, IMP-6 and the "Prognoz-2" station) and for relativistic energies (neutron monitor data) virtually simultaneously at 1400-1500 UT on 4 August. The moment of injection of cosmic rays on the sun, according to data from high-latitude neutron monitors, is determined by the author at 1200 UT on 4 August. No relativistic nuclei ($E_{kin} \geqslant 600$ MeV/nucleon) with charges $Z \geqslant 6$ and $Z \geqslant 15$ were generated in the flare of 4 August with an accuracy $\sim 10\%$ of the value of the corresponding background fluxes of nuclei, although nuclei with an energy of several tens of MeV per nucleon were registered by a number of researchers ("Prognoz," "Geos-2," photoemulsions on rockets, etc.).

The circumstance that according to data from the ground network of stations the effect of an increase in SCR was discovered only after 1200 UT on 4 August was attributable, in our opinion, to the following phenomena. First, the increase in the intensity of SCR, according to [3], occurred gradually. Second, during this same period of time the decrease in the intensity of GCR continued. Third, the magnitude of the anticipated effect in the high-latitude neutron monitors is small ($\sim 1\%$), and the anisotropy is also small [1, 2]. Therefore, only a further approximately fivefold increase in the intensity of protons with an energy $E_{kin} \geqslant 500$ MeV (data from the "Prognoz-2" station) was reliably registered by the high-latitude neutron monitors.

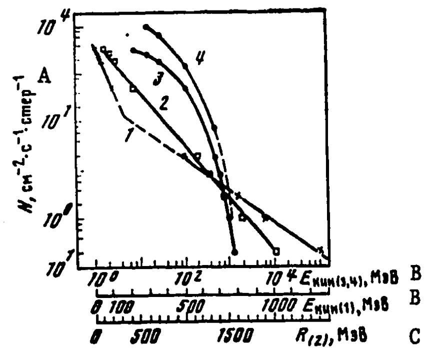

Fig. 2. Integral spectra of solar protons on the basis of data from measurements aboard the "Prognoz-2" station on 4 August 1972. 1, 2) in exponential form for 1200 UT for energy (1) and for hardness (2); 3, 4) in power-law form for energy for 1200 UT (3) and 1500-1800 UT (4); the dashed lines represent extrapolation of experimental data.

KEY:

A. ...sec...sr
B. E_{kin}...MeV
C. MeV

Figure 2 shows integral spectra of solar protons for different moments in time. For 1200 UT the proton spectrum is represented by three methods: three scales are plotted along the x-axis -- a logarithmic scale for kinetic energy and for hardness (rigidity) (R). It can be seen that the spectrum with sufficiently good accuracy can be represented in the form $J(\geqslant P) - Ae^{-P/P_0}$, where P_0 = 200 mV in the rigidity range 0.2-2GV. It must be noted that the magnitude of the flux of protons with an energy $\geqslant$ 500 MeV for 1500-1800 UT exceeds by two orders of magnitude the corresponding value obtained in [6] on the basis of an analysis of neutron monitor data. The reason for this discrepancy is evidently associated with the incorrect values of the coupling coefficients used in [6].

Unusual Increase in the Cosmic Ray Flux ("Tube") of 5 August 1972

On 5 August in the phase of restoration of the intensity of cosmic rays after the flare and Forbush effects of 4 August, during the period 0300-0500 UT (according to measurements on the "Prognoz" stations, IMP satellites, etc.), there was a rather rare phenomenon: an increase in the intensity of cosmic rays with rather sharp leading and trailing fronts (Figs. 3, 4). This increase has the following unusual characteristics:

1) the spectrum is rather hard, with an exponent of the integral spectrum in the case of a power-law representation $\sim$1.5 for E of the order of several tens of MeV per nucleon;

2) the upper energy limit of the increase, estimated on the basis of data from surface meson telescopes, is $\sim$ 50-60 GeV [1];

A

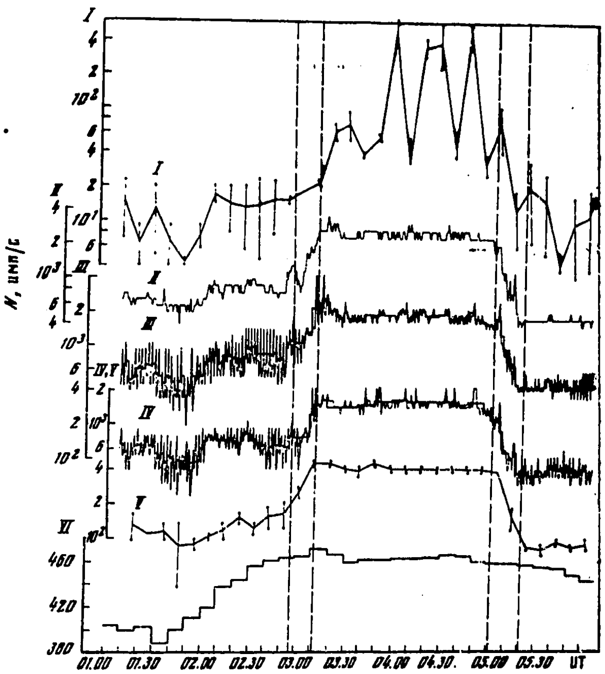

Fig. 3. Increase in differential fluxes of cosmic rays on 5 August 1972 (data from measurements on "Prognoz-2" station). I-V) protons: I) E_p = 0.1-0.5 MeV perpendicular to the earth-sun line (φ = 90°); E_p = 1-5 MeV, II) from sun (φ = 0°), III) φ = 90°, IV) toward sun (φ = 157°), V) E_p = 15-30 MeV (φ = 90°), VI) data from neutron monitor (Tiksi Bay); dashed lines -- limits of increase fronts. A) N, pulses/sec

3) the increase begins virtually simultaneously for particles with different energies (with an accuracy to the values corresponding to the Larmor radius of particles in the field $H \sim 40\gamma$, such fields were registered on the satellite "Explorer-41" [7] before and after the "tube");

4) the energy density of particles at 0400 UT$\approx 7 \cdot 10^2$ eV/cm^3 (middle of "tube"), and the energy density of the magnetic field outside the "tube" $B^2/8\pi$ = $2.484 \cdot B^2 = 4 \cdot 10^3$ eV/cm^3 (field B = 40γ);

5) the flux of protons 1-5 MeV during the period 0100-0600 is sharply anisotropic. The nature of the anisotropy outside and inside the "tube" is different. In the "tube" there is registry of a flux of particles from the sun with an anisotropy of 20%. Outside the "tube" there is registry of a flux of protons with an anisotropy $\sim$30% by a detector situated at an angle φ = 90° to the earth-sun line;

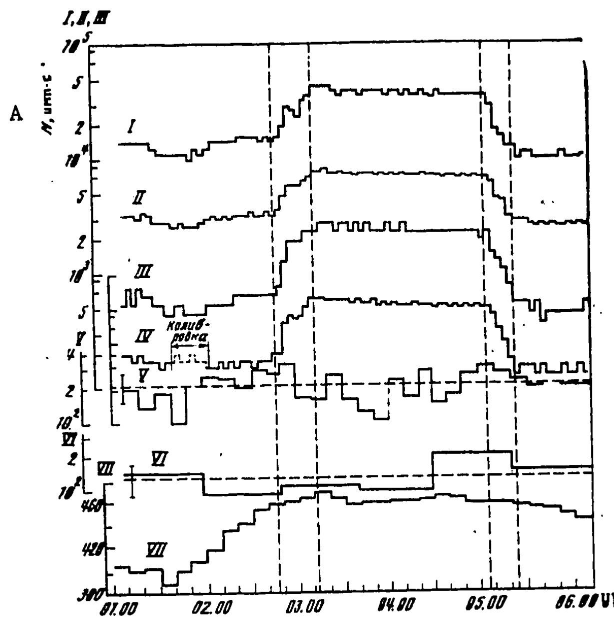

Fig. 4. Increase in integral fluxes of cosmic rays on 5 August 1972 (data from measurements aboard "Prognoz-2" station). I-IV) protons: I) $E_p > 15$ MeV, II) $E_p > 30$ MeV, III) $E_p > 100$ MeV, IV) $E_p > 500$ MeV, V, VI) $E_p \geqslant 600$ MeV/nucleon: nuclei $Z \geqslant 6$ (V), $Z \geqslant 15$ (VI); VII) data from neutron monitor (Tiksi Bay); vertical dashed lines -- limits of increase fronts; horizontal dashed lines -- mean values. A) N, pulses•sec

6) for high-energy particles (data from neutron monitors [1]) the anisotropy is $\sim 5\%$ with the direction from the sun;

7) the intensities of cosmic rays to the "tube" and after it, according to data from satellite measurements, are equal to one another;

8) for protons with an energy 1-5 MeV, registered by a detector looking at the sun ("Prognoz-2"), before the beginning of the tube there is a brief (~ 10 min) increase. A similar increase is observed for higher-energy protons on the basis of data from instruments situated on the moon ("Apollo-12, -14, -15" [4]) and can be seen up to energies $\geqslant$ 500 MeV on the basis of data from the "Prognoz-2" station;

9) the onset of this brief increase, and also the intensity maximum of cosmic rays in the "tube" are attained aboard the "Prognoz-2" station 5-6 minutes earlier than for the instruments on the moon. At the same time,

the decrease in intensity (trailing edge of the "tube") according to instruments on the "Prognoz" stations occurs later by these same 5-6 minutes. The projections of the moon and the orbit of the "Prognoz-2" stations onto the plane of the ecliptic are shown in Fig. 5. The solar ecliptic coordinates at 0400 UT on 5 August for the "Prognoz-2" station were: $X = 11.3\ R_E$: $Y = -7.9\ R_E$; $Z = 13.3\ R_E$ (R_E = 6,370 km, X = 72,000 km, Y = -50,000 km, Z = 84,000 km); for the moon: X_m = 218,000 km; Y_m = -280,000 km; Z_m = 19,350 km; X -- direction to the sun; Z -- directed perpendicular to the plane of the ecliptic;

10) an absence of an increase for GCR nuclei with an energy $E_{kin} \geqslant 600$ MeV/nucleon with charges $Z \geqslant 6$ and $Z \geqslant 15$ in the presence of a threefold increase in the intensity of protons with $E_{kin} \geqslant 500$ MeV (data for "Prognoz-2" station);

11) in the "tube" itself there is a gradual decrease in the intensity of cosmic rays; the rate of decrease increases with an energy increase.

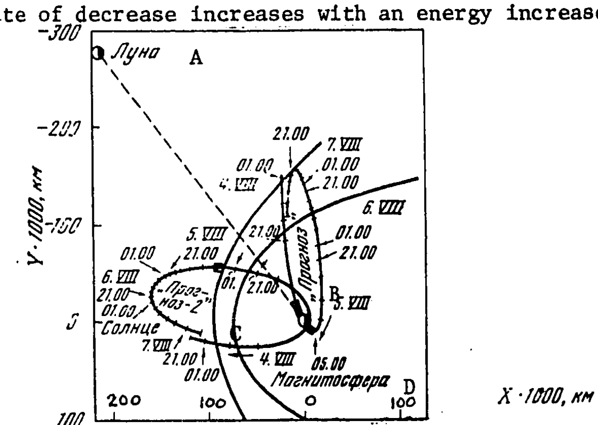

Fig. 5. Projections of moon at 0400 UT on 5 August 1972 and orbit of "Prognoz" and "Prognoz-2" stations onto plane of the ecliptic in solar ecliptic coordinates. The shaded sectors correspond to the period 0300-0500 UT.

KEY:

A. Moon
B. Prognoz
C. Prognoz-2
D. Magnetosphere

The enumerated principal characteristics indicate the complexity and unusualness of the observed increase effect, requiring further study. However, some conclusions can be drawn even now. For example, points 3), 4) indicate that in this case we are dealing with a spatially limited magnetic trap containing protons up to an energy ~50 GeV. At the same time, point 7) does not agree with the model proposed in [1], and point 10) with the model in [2]. Points 7-9) can give information on the spatial configuration of the registered trap.

BIBLIOGRAPHY

1. Agrawal, S. P., Ananth, A. G., Bemalkhedkar, M. M., et al., JGR, 79, 2269, 1974.

2. Panerantz, M. A., Duggal, S. P., JGR, 79, 913, 1974.

3. Volodichev, N. N., Grigorov, N. L., Kolesov, G. Ya., et al., KOSMICHESKIYE ISSLEDOVANIYA (Space Research), 12, No 3, 483, 1974.

4. WORLD DATA CENTER A FOR SOLAR-TERRESTRIAL PHYSICS, REPORT UAG-28, Part II, 1973.

5. Dorman, L. I., VARIATSII KOSMICHESKIKH LUCHEY I ISSLEDOVANIYE KOSMOSA (Variations in Cosmic Rays and Space Research), Moscow, Izd-vo AN SSSR, p 292, 336, 1963.

6. Lockwood, Y. A., Webber, W. R., Hsieh, L., JGR, 79, 4149, 1974.

7. Venkatesan, D., Mathews, T., Lanzerotti, L. Y., et al., JGR, 80, 1715, 1975.

[8144/1843-5303]

5303
CSO: 8144 / 1843

INVESTIGATION OF THE EARTH'S PLASMOSPHERE USING TRAPS ABOARD THE 'PROGNOZ' AND 'PROGNOZ-2' STATIONS

Moscow PROBLEMY SOLNECHNOY AKTIVNOSTI I KOSMICHESKAYA SISTEMA "PROGNOZ" in Russian 1977 pp 184-195

[Article by V. V. Bezrukikh, G. I. Volkov, K. I. Gringauz and V. S. Mokrov]

[Text] This article describes the apparatus used and the method employed in the processing of experimental data relating to determination of the concentration and temperature of cold ions of the plasmosphere and gives some results obtained aboard the "Prognoz" and "Prognoz-2" stations.

Both stations carried a complex of wide-angle detectors for investigating low-energy plasma in the magnetosphere and in interplanetary space in the energy range from 1 eV to 4.2 keV [1].

1. Apparatus

Stations of the "Prognoz" series in flight were oriented on the sun with an accuracy to 10°. Three traps were mounted on the illuminated side of the "Prognoz" and "Prognoz-2" stations: a modulation trap T_1 and two integral traps (plane trap T_2 and hemispherical trap T_3). On the opposite side from the sun on each station there was one hemispherical trap T_4. The axes of symmetry of the traps were parallel to the longitudinal axis of the stations (Fig. 1).

The collector current of the trap T_2 could be created by ions with energies $E_i > 40$ eV and electrons with $E_e > 70$ eV and the current for the trap T_3 by ions with $E_i \geqslant e\varphi$ (φ is station potential relative to plasma) and electrons with $E_e > 70$ eV. In addition, a contribution to the currents of the integral traps, illuminated by the sun, came from the photoemission from parts of the trap situated within it. The photoelectric component of the trap current changed insignificantly as a result of small variations in orientation of the trap relative to the direction toward the sun and can be determined in a comparison of readings of the traps T_1 and T_3, obtained during the time of station flight in undisturbed interplanetary space.

The current variations registered by trap T_3 and the absence of current variations of commensurable amplitude for trap T_2 have been interpreted as variations of the flux of thermal ions.

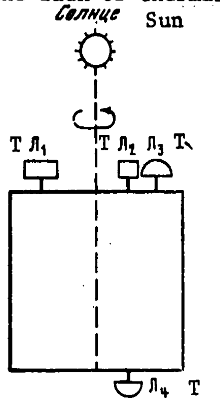

Fig. 1. Positioning of traps on "Prognoz," "Prognoz-2" stations for registry of ions with $e\varphi_s < E \leqslant 4200$ eV (T_1); with $E_i \geqslant 40$ eV (T_2) and $E_i > e\varphi_s$ (T_3, T_4).

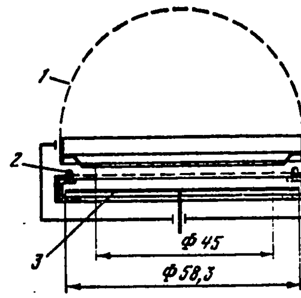

Fig. 2. Diagram of hemispherical trap. 1) grid C_1 (potential 0 V; 2) grid C_2 (potential 70 V); 3) collector (potential 20 V)

In order to determine the ion concentration we used readings of the shaded trap T_4, free of a photocurrent, for which the angle of attack (the angle between the axis of symmetry of the trap and the direction of station flight) was at the same time more favorable in the course of the greater part of the period of active existence of both stations than for the illuminated trap.

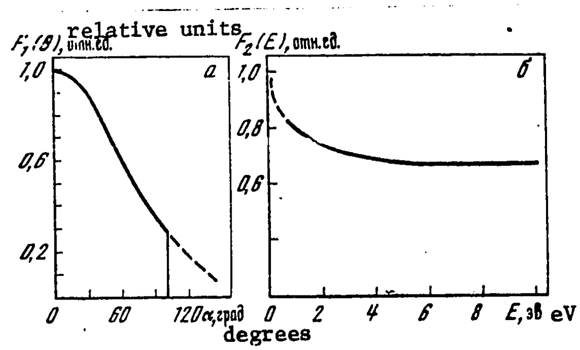

Fig. 3. Angular characteristic curve (a) of hemispherical trap (solid curve -- taking into account the shading of the field of view of the trap by the station body) and dependence of the trap current on ion energy (b) (dashed line -- result of extrapolation when 0.1 eV$\leqslant$E$\leqslant$3 eV).

A diagram of a hemispherical trap is shown in Fig. 2. The outer grid of trap C_1 was fabricated from a nickel "screen" with a transparency coefficient 0.75. The suppressor grid C_2 was fabricated from gold-tungsten wire with a diameter 0.02 mm, galvanically attached in a Kovar ring. The grid transparency coefficient is 0.98. The collector is a stamped nickel plate with a thickness 0.08 mm.

The presence of a considerable negative potential across the grid C_2 (-70 V) creates a field in the space between the two grids; this effectively attracts to the collector positive ions with energies $E_i \approx 1$ eV, arriving at the outer grid with angles of attack $\alpha < 120°$ (α is the angle between the direction of the flight of the particle and the axis of the trap).

The characteristics and parameters of the hemispherical traps, necessary for computing the concentrations and temperatures of ions on the basis of the currents measured by the trap, were investigated experimentally. For this purpose the trap was placed in a vacuum chamber in which a pressure $\sim 3 \cdot 10^{-6}$ mm Hg was maintained and was irradiated by low-velocity fluxes of Ar^+ ions with the parameters: 1) mean energies E_0 of the ion beams 3 eV E_0 10 eV; 2) scatter of a beam of ions by energies E_{max}/E_0 = 0.1-0.15; 3) beam current $J = 2 \cdot 10^{-8}$ A; 4) decrease in density of beam current from its axis to a distance equal to the radius of the outer wall of the trap, 5%.

In a laboratory experiment we measured the current in the circuit of the trap collector when it is irradiated by ion beams with angles between the axis of symmetry of the trap and the direction of the ion flux $0° \leqslant \alpha \leqslant 180°$ for the mean energies of the beams 3 eV$\leqslant E \leqslant$10 eV. The characteristics of the trap for ions $E < 3$ eV were obtained from the similarity relationships for E = 3 eV and a multiple increase in potentials across its electrodes.

As indicated by a laboratory experiment, the instrument function $F(\theta, v)$ of the trap (that is, the dependence of the current registered by it on the angle of arrival of the ions relative to the axis of symmetry of the trap θ and ion velocity v) for ions with energies $E \leqslant 10$ eV can be represented in the form $F(\theta, v) = F_1(\theta) F_2(v)$. Curves of the functions F_1 and F_2 are illustrated in Figure 3,a and b. The width of the trap diagram $F_1(\theta)$ at the 0.1 level is $\sim 130°$. However, in flight the angular diagram was limited by the body of the station to 100°.

The function F_2 characterizes the dependence of the trap current on ion energy for ions entering into the trap. Figure 3,b shows that with an ion energy $E_i < 3$ eV there is some increase in the function F_2, evidently determined by an increase in the effectiveness of focusing of ions by the field of the grid C_2 with a decrease in particle energy.

2. Method for Processing Data

Now we will examine a method for processing trap measurements on the assumption that the station potential is

$$\varphi \ll \frac{kT_i}{e}, \qquad (1)$$

where k is the Boltzmann constant; e is electron charge; T_i is ion temperature.

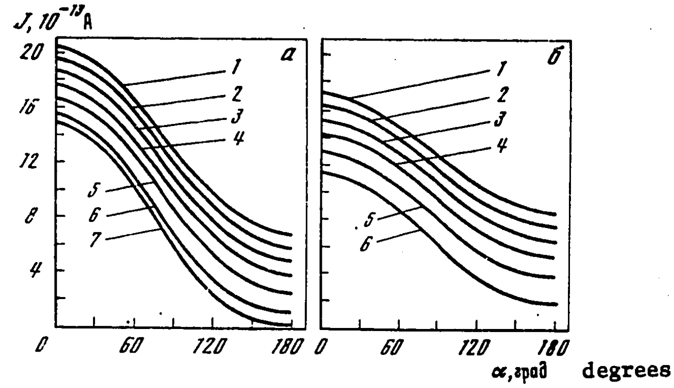

Fig. 4. Dependence of the current j (V, T, α) registered by a trap when n - 1 ion/cm^3 on ion temperature T_i and the angle of attack α for a station velocity V - 8 km/sec (a) and V - 5 km/sec (b)

We will denote by j the current which the trap registers with an ion concentration $n_i = 1$ ion/cm^3; then with a concentration n_i the trap registers the current $J = jn_i$.

In a coordinate system moving with the station, with a Maxwellian velocity distribution and $\varphi \ll kT_i/e$

$$j = e\left(\frac{m_i}{2kT}\right)^{3/2} S \int_0^{v_1}\int_0^{\theta_0}\int_0^{2\pi} F_1(\theta) F_2(v) v^3 \exp\left\{-\frac{m}{2kT_i}\left[v^2 + V^2 - 2vV(\sin\alpha\sin\theta\cos\varphi - \cos\alpha\cos\theta)\right]\right\}\sin\theta\, dv\, d\theta\, d\varphi, \quad (2)$$

where m is the ion mass; S is the trap aperture area; V is station velocity; $F_1(\theta)$ is the angular characteristic of the trap; $F_2(v)$ is a function characterizing the dependence of the trap current on ion velocity; v is ion velocity in a fixed coordinate system; θ, φ are the coordinate angles.

The upper limit of the first integral in formula (2) $v_1 = 4(kT/m)^{1/2}$. The upper limit of the second integral θ_0 is the width of the angular diagram, taking into account its shading by the station body (for traps T_3 and T_4, mounted on the "Prognoz," "Prognoz-2" stations, $\theta_0 = 100°$).

The j values were computed on an electronic computer for temperatures $2\cdot10^3$ K$\leqslant T_i \leqslant 25\cdot10^3$K, a station velocity $3\cdot10^5$ cm/sec$\leqslant V \leqslant 10^6$ cm/sec and angles of attack $0° \leqslant \alpha \leqslant 180°$ (see Fig. 4).

Due to the fact that according to estimates of T_i in the plasmosphere on the stations "Elektron-2" [2, 3] and "Prognoz" [see article on page 196 in this collection of articles], and also measurements on the OGO-5 satellite

[4], $T_i \approx 10^4$K, computations of n_i according to data from the trap T_4 on the "Prognoz" and "Prognoz-2" stations were made on the assumption that $T_i = 10^4$K. As indicated by estimates, the possible errors in determining n_i, associated with the difference in the real ion temperatures from $T_i = 10^4$K, do not exceed the coefficients $n_{i\ max}/n_{i\ min} \leqslant 1.5$ with $4 \cdot 10^3\text{K} \leqslant T_i \leqslant 20 \cdot 10^3\text{K}$ and $0° \leqslant \alpha \leqslant 90°$.

The ion concentration n_i was computed with an electronic computer from the expression

$$n_i = J_{\text{изм}}/j\,(\alpha, V)/_{T_i = 10^4\text{K}} \quad (3)$$

[ИЗМ = meas] for each measured current value J_{meas}, taking into account the real value of the angle of attack and station velocity V. The angle of attack α_1 of the trap T_4, mounted on the shaded side of the "Prognoz" station, was determined from orbital data using the formula

$$\alpha_1 = \arccos\,(-\,V_{XSE}/V), \quad (4)$$

where V_{XSE} is the projection of satellite velocity onto the X axis in a solar-ecliptic coordinate system; V is the station velocity modulus. The angle of attack for the trap T_3, mounted on the illuminated side of the "Prognoz" station, is

$$\alpha_2 = 180° - \alpha_1. \quad (5)$$

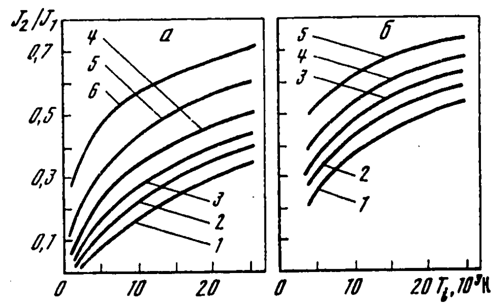

Fig. 5. Dependence of ratio of currents for traps T_3, T_4, situated on the "Prognoz" station, on ion temperature and angle of attack α_1 of trap T_4 for α_1: 1) 0°, 2) 30°, 3) 40°, 4) 50°, 5) 60°, 6) 70°

The error in determining the angles of attack, associated with inaccuracy in maintaining station orientation, in the "Prognoz" case was $\leqslant 10°$ and for the "Prognoz-2" -- $\sim 20°$. However, due to the broad angular diagram of the traps, the error n_i, associated with uncertainty of the angle of attack, was $\sim 20\%$ in the first case and $\sim 40\%$ in the second.

For determining n_i the measured values of the current for the trap T_4 as a function of time $J_{meas}(t)$ and the station velocities V(t) and its projection onto the X-axis in a solar-ecliptic coordinate system $V_{XSE}(t)$ were introduced into the electronic computer memory. Excluding time, for each J_{meas} the V and V_{XSE} values were appropriately introduced and the angle of attack was determined with (4) and (5) taken into account. Finally, using a $j(V, \alpha)$ table for known V and α, precomputed and introduced into the computer memory, we determined the j value, after which n_i was determined from (3).

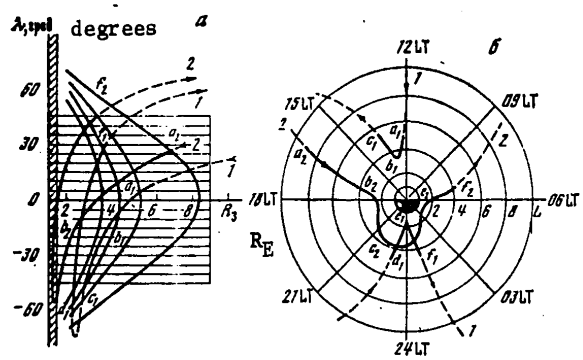

Fig. 6. Projection of orbits of "Prognoz" station on 20 May 1972 (1) and "Prognoz-2" station on 7 July 1972 (2) onto meridional plane in geomagnetic coordinates R_E, λ and onto equatorial plane in coordinates R_E, LT. The dashed lines are segments of trajectories passing outside the plasmosphere, the solid lines are for trajectories passing within the plasmosphere R_E, LT.

It follows from (2) that the ion current, registered by the integral trap, on the assumption of a Maxwellian velocity distribution of ions, is dependent on ion temperature. With a station velocity $V \sim (2kT/m)^{1/2}$ (specifically this relationship of velocities is observed in the plasmosphere) in order to determine T_i it is possible to use a method based on the dependence of the trap current on the angle of attack α. If we have two current values, J_2 and J_1, measured with two known values of the angles α_1 and α_2 in the course of a sufficiently short time interval in order to assume n_i and T_i to be constant, it is possible to find T_i from the ratio

$$J_2/J_1 = j_2(\alpha_2, T_i)/j_1(\alpha_1, T_i).$$

As the two current measurements it is possible to use both measurements made with one trap on a rotating space vehicle and measurements made using two traps on a stabilized vehicle, but differently oriented relative to the velocity vector.

The values $j(T_i, \alpha, V)$, obtained as a result of computations, and the relationship between the angles of attack of the traps T_3 and T_4, mounted on the "Prognoz" station, make it possible to obtain the dependence of T_i on the ratio of the currents for the two traps J_2/J_1. Examples of the dependence

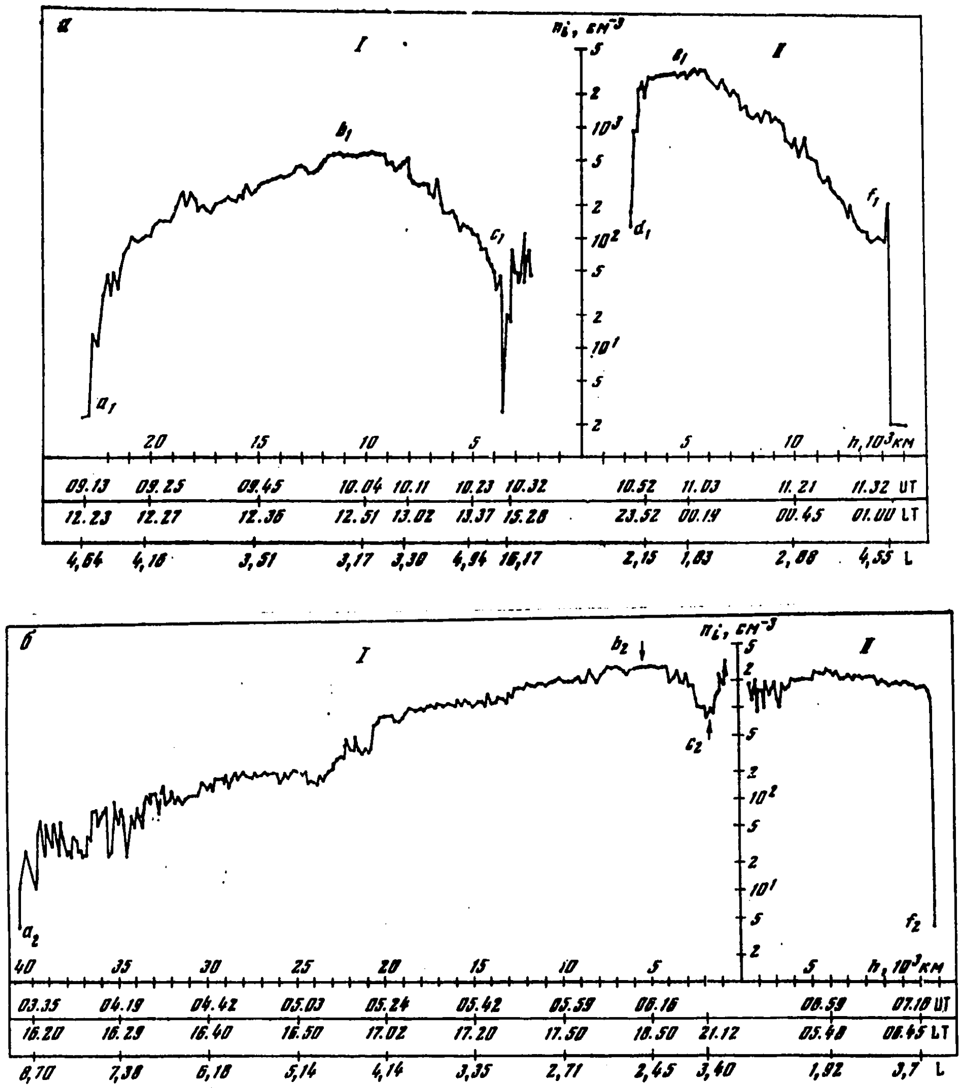

Fig. 7. Concentration of ions n_i in plasmosphere measured by trap T_4 on "Prognoz" station on 20 May 1972 (a) and on "Prognoz-2" station on 7 July 1972 (b) on descending (I) and ascending (II) segments of orbit. The letters denote the points where the "Prognoz" (subscript 1) and "Prognoz-2" (subscript 2) stations intersect the plasmopause (a, c, d, f) and the geomagnetic shells with minimum values of the L-parameter (b, e).

J_2/J_1 (or j_1, j_2, which is the same thing) on ion temperature for $0° \leqslant \alpha \leqslant 60°$ are given in Fig. 5.

Figure 5 shows that the accuracy in determining T_i from the known ratio J_2/J_1 decreases with an increase in α_1. In this article the ion temperature was determined for $T_i \leqslant 25\ 000$ K in the range of angles $\alpha_1 = 0-35°$ (in this case $\alpha_2 = 180-145°$); in the future plans call for carrying out determinations of ion temperature also for $T_i > 25\ 000$ K.

The adopted limitations on the angle α_1 made it possible to determine T_i only in the daytime part of the plasmosphere, whereas limitations on ion temperature in some regions of the plasmosphere made it possible to determine only the lower limit of possible T_i values.

If it is assumed that the error in measuring T_i is determined by the errors in measuring J_2 and J_1 and an inexact knowledge of the α value, it can be demonstrated that the relative error in determining T_i during the period from 8 through 20 May 1972, when $\alpha_1 < 30°$, with $T_i \sim 25\ 000$ K was $\delta T_i/T_i \approx 10\%$, whereas during the period from 17 through 25 June 1972, when $\alpha_1 = 30-35°$, $\delta T_i/T_i \approx 25\%$.

It should be noted that for determining T_i on the basis of data registered by the traps T_3 and T_4 on the "Prognoz" station it is necessary to introduce first a correction for the photocurrent into the readings of the trap T_3, illuminated by the sun. This correction is determined from a comparison of the currents of the illuminated trap T_3 and the modulation trap T_1 in interplanetary space. The photocurrent of the trap T_3 is $J_{ph} = J - J_p$, where J is the current measured by the hemispherical trap, J_p is the value of the ion currents of the solar wind, measured by the modulation trap T_1, whose readings are virtually free of a photocurrent, reduced to the dimensions of the trap T_3.

3. Measurement Results

The near-earth segment of the "Prognoz" and "Prognoz-2" orbits is shown in Fig. 6,a,b (R_E is geocentric distance, λ is geomagnetic latitude, L is the geomagnetic shell parameter, LT is local time). The lines of force of the geomagnetic field (in a dipole approximation) are shown in Fig. 6,a in the form of a family of curves. The horizontal shading denotes the region with $\lambda \leqslant 45°$, beyond whose limits the high-apogee American satellites (IMP-2, OGO-1, -3, -5, C^3A), outfitted with instruments making it possible to register cold plasma in the plasmosphere [4-10], did not penetrate. The oblique shading denotes the region in which measurements were made of the plasma concentration on polar and high-latitude satellites with an apogee $\leqslant$ 3000 km: "Explorer-32," OGO-6, "Kosmos-378," ISIS-1 [11-15].

The peculiarities of orbits of stations in the "Prognoz" series made it possible not only for the first time to obtain information on the ion concentration in the region of the plasmosphere with the coordinates $R > 1.5R_E$

and $\lambda > 45°$, but also in the course of relatively short time intervals (1-2 hours) to obtain data on the ion concentration in sectors of the geomagnetic shells $3 \leqslant L \leqslant 7$ both distant from and close to the earth.

During many revolutions of both stations around the earth during the period from 18 April through 25 November in the course of about four hours they intersected the plasmopause four times in one revolution: twice in the descending segment of the orbit and twice on the ascending segment. The total number of the orbits of both stations in which plasmospheric ions were measured exceeds 60.

Figure 7,a,b shows data on the n_i distribution in the plasmosphere, obtained on the "Prognoz" on 20 May 1972 and on the "Prognoz-2" on 7 July 1972. The $n_i(L)$ distribution, measured on 20 May, is characteristic for a plasmosphere greatly deformed by the strong magnetic storm of 15 May 1972 when the K_p index attained 8_+.

On the descending segment of the orbit on 20 May the "Prognoz" intersected the plasmopause at 0913 UT, approximately at midday LT, at an altitude of 22 700 km ($L \simeq 4.6$) in the plane of the geomagnetic equator (point a_1 in Figures 6 and 7, a, I). The ion concentration in the plasmosphere near the plasmopause was ~ 50 ions/cm^3. The approach of the station to the earth to an altitude 10 000 km (point b_1 in Figures 6 and 7,a,I) was accompanied by a decrease in the values of the L-coordinate from 4.6 to 3.15. The value of the ion concentration increased to $n_i = 6 \cdot 10^2$ ions/cm^3. With a further approach of the station to the earth in the segment 10 000 km$>h>$3500 km the L-coordinate increased to L = 11 and the trap registered a decrease in n_i.

Figures 6 and 7,a show that the plasmopause (c_1) was repeatedly intersected in the interval of 1330-1500 LT at altitudes 5000 km$>L>$3500 km ($5<L<11$). A more precise determination of the position of the plasmopause at altitudes $<$ 5000 km according to data obtained on the "Prognoz," "Prognoz-2" stations is difficult as a result of the low frequency of interrogation of the telemetric system (once in 41 sec) in comparison with the velocity of intersection of the L-shells by the stations at these altitudes.

The currents registered by the T_4 trap in the segment 3500-2700 (corresponding to the mentioned altitudes: L-coordinates 12, 28, 12; LT about 15, 18, 22) were evidently formed either by leaking protons with an energy ~ 1 keV or by fluxes of solar wind protons.

In the immediate neighborhood of the perigee, whose altitude on the considered revolution was 2368 km, in the course of 2 min at $6.3<L<8.7$ the trap registered currents close to the limit of instrument response. The n_i values did not exceed several units per cubic centimeter.

On the ascending segment of the revolution the plasmopause was intersected a third time at an altitude of 2370 km ($L \cong 5$) at 1044 UT and $\sim$2300 LT. The ion concentration near the plasmopause was $n_i = 10^2$ ions/cm^3. With an increase in altitude by only 300 km (but with a decrease in the L-parameter from 5.0 to 2.1) n_i increased by a factor of more than 10 and at $h \simeq 2570$ km $n_i = 3 \cdot 10^3$ ions/cm^3. At altitudes 2370 km $< h <$ 4500 km, where the coordinate attained a minimum value L = 1.8, the ion concentration increased slowly to $4 \cdot 10^3$ ions/cm^3. With a further increase in altitude and the L-coordinate the ion concentration changed, to $n_i = 10^2$ ions/cm^3 at an altitude h = 14 540 km (L = 4.6); here at 1138 UT and $\sim$0100 LT the station for a fourth time passed through the plasmopause.

During the first period of its life the "Prognoz-2" orbit considerably differed from the "Prognoz" orbit on 20 May 1972. However, already late in July 1972, as a result of evolution of the "Prognoz-2" orbit, the same as in the case of the "Prognoz," approaching the earth, intersected extremely remote L-shells.

The data on the ion concentration in the plasmosphere, cited in Fig. 7,b, were obtained on the "Prognoz-2" on 7 July 1972 during the time interval 0325-0720 LT.

The first intersection of the plasmopause by the "Prognoz-2" station occurred at an altitude $h \simeq 40\ 000$ km near the plane of the galactic equator (L = 8.7, point a_2 in Fig. 6,a,b; 7,b). At an altitude $h \simeq 6000$ km (point b_2 in Fig. 6,a,b; 7,b; L = 2.5) the ion concentration attained the maximum $n_i = 2 \cdot 10^3$ ions/cm^3 and with further approach of the station to the earth (but with an increase in the L-coordinate) began to decrease and attained the minimum $n_i = 8 \cdot 10^2$ ions/cm^3 at L = 3.4 (point c_2 in Fig. 7,b). With increasing distance of the station from the earth the ion concentration, according to the trap readings, changed insignificantly up to the clearly expressed plasmopause, which the station intersected at an altitude h = 11 000 km (L = 4.1; $\sim$0640 LT) at 0716 UT (point f_2 in Fig. 6,a,b; 7,b).

The measurements made by the traps on the "Prognoz" station during the period from 22 April through 20 July 1972 were used for determining the ion temperature in the daytime sector of the plasmosphere by the method described above.

Detailed data on the ion temperature in the plasmosphere are given in an article in this collection of papers [p 196]. We note here that according to preliminary data, on 22 April 1972, at altitudes 4000-16 000 km ($2.5 < L < 3.6$) the ion temperature changed from 3000 to 10 000 K.

BIBLIOGRAPHY

1. Bezrukikh, V. V., Belyashin, A. P., Volkov, G. I., et al., GEOMAGNETIZM I AERONOMIYA (Geomagnetism and Aeronomy), 14, No 3, 399, 1974.

2. Gringauz, K. I., Bezrukikh, V. V., Breus, T. K., KOSMICHESKIYE ISSLEDOVANIYA (Space Research), 5, No 2, 245, 1967.

3. Bezrukhikh, V. V., Breus, T. K., Gringauz, K. I., KOSMICHESKIYE ISSLEDOVANIYA, 5, No 5, 798, 1967.

4. Serbu, G. P., Maier, E. J. R., JGR, 75, 6103, 1970.

5. Taylor, H. A., Brinton, H. C., Jr., Smith, C. R., JGR, 70, 5769, 1965.

6. Taylor, H. A., Brinton, H. C., Pharo, M. W., JGR, 73, 961, 1968.

7. Binzack, J. H., JGR, 72, 5231, 1967.

8. Brinton, H. C., Pickett, R. A., Taylor, H. A., Jr., PLANET. SPACE SCI., 16, 899, 1968.

9. Chappel, C. R., Harris, K. K., Sharp, G. W., JGR, 75, 50, 1970.

10. Maynard, N. C., Kauffman, D. P., REPORT X-645-72-201, Goddard Space Flight Center.

11. Donley, J., Brace, L. H., Findley, J. H., et al., PROC. IEEE, 57, 1078, 1969.

12. Taylor, H. A., Walsh, W. I., JGR, 77, 6716, 1972.

13. Gringauz, K. I., Gdalevich, G. L., Khokhlov, M. Z. et al., SPACE RES., XII, 549, 1973.

14. Whittaker, J. H., Brace, L. H., Burrows, J. R., et al., JGR, 77, 6121, 1972.

15. Brace, L. H., Theis, R. F., JGR, 79, 1871, 1974.

[8144/1843-5303]

5303
CSO: 8144 / 1843

DEPENDENCE OF POSITION OF THE FRONT OF THE CIRCUMTERRESTRIAL SHOCK WAVE AND THE MAGNETOPAUSE ON PARAMETERS OF THE SOLAR WIND AND PLASMA STRUCTURE OF THE MAGNETOPAUSE ACCORDING TO DATA FROM THE CHARGED PARTICLE TRAPS ABOARD THE 'PROGNOZ' AND 'PROGNOZ-2' STATIONS

Moscow PROBLEMY SOLNECHNOY AKTIVNOSTI I KOSMICHESKAYA SISTEMA "PROGNOZ" in Russian 1977 pp 242-255

[Article by V. V. Bezrukikh, T. K. Breus, M. I. Verigin, P. A. Maysuradze, A. P. Remizov and E. K. Solomatina]

[Text] The "Prognoz" and "Prognoz-2" stations carried sets of ion traps for measuring the characteristics of ions in the solar wind and earth's magnetosphere. Each of these sets included a modulation trap for measuring the differential spectrum of ions in the energy range 0-3.85 keV and three integral traps. The modulation and two integral traps were oriented on the sun; one integral trap was oriented in an antisolar direction. Measurements of the ion fluxes by means of the modulation trap were made in eight energy ranges (0-0.03, 0-0.22, 0.22-0.36, 0.36-0.58, 0.62-0.94, 1.0-1.48, 1.58-2.53, 2.8-3.85 keV). The time interval between interrogation of the energy intervals was $\sim$40.8 sec; therefore, the full spectrum of ions was registered in 5.44 minutes. The integral traps registered the sum of the flux of ions with an energy $E > \max(0, e\varphi_k)$, where φ_k is the station potential, and the flux of electrons with an energy > 70 eV; they were also interrogated once in 40.8 sec. A detailed description of the apparatus and sensors was given in [1].

In this article we analyze the results of measurements made using modulation traps in the shock wave region and in the magnetopause region aboard the "Prognoz" and "Prognoz-2" stations during April-October 1972 (from 29 July through 17 September -- the results of simultaneous measurements). The data from the integral ion traps were used only for refining the times of intersections of the magnetopause and the shock wave front because they were obtained with a greater time resolution than the data from the modulation traps.

1. Investigation of Variations of Position of Shock Wave Front and Magnetopause

Simultaneous measurements in the solar wind and magnetosphere aboard two or more vehicles is interesting and for the time being is still a relatively rare possibility for studying the correlation of different processes. Accordingly, for investigating variations in the position of the shock wave front and magnetopause use is made precisely of data from simultaneous measurements aboard the "Prognoz" and "Prognoz-2" stations.

Intersections of the shock wave front and the magnetopause by these stations were registered on the basis of the characteristic change in the form of the modulation trap spectra and changes in the current registered by the integral traps. In the transition region the modulation traps register the broadening of the ion spectrum in comparison with the solar wind and displacement of the spectral maximum to lower energies. Thermalization (and accordingly, an increase in the flux) of electrons and a decrease in the transport velocity of ions has the result that in the transition region the currents of the integral traps become negative. In the earth's magnetosphere, near its boundary, the level of the currents registered by both the modulation and integral traps decreases sharply and is close to the response threshold of the traps [2].

The intersections of the shock wave front and magnetopause observed by one of the stations were compared with the changes in these boundaries computed using data on the dynamic pressure of the solar wind obtained at the other station; the results of the comparison are shown in Figures 1-3. Descriptions of the figures are given below. How the comparison was made will be discussed below.

It follows from gas-dynamical computations that with sufficiently great values of the Mach numbers the distance to the shock wave front R_S and the magnetopause R_M (with a not too great angular distance φ of the current point from the direction to the sun) can be written approximately in the following form:

$$R_{S,M} = C_{S,M} (\rho V^2)^{-1/6} f_{S,M}(\varphi), \tag{1}$$

where C = const, ρ is density and Y is the velocity of the solar wind; $f(\varphi)$ is a factor describing the configuration of the front or magnetopause. It can be seen from formula (1) that with φ= const the change in the distance to the boundary is dependent only on the change in the dynamic pressure of the solar wind ρV^2.

In order to exclude the relative change in the positions of the investigated boundaries and stations, associated with a change in the φ angle, occurring during motion of the stations in orbit, in each of the analyzed time intervals the segments of the station orbits were reduced to one and the same angular value. For this purpose use was made of the configuration

$f_{S,M}(\varphi)$ of the mean front of the shock wave and magnetopause, computed on the basis of all the registered intersections (Fig. 4). A similar transformation of the trajectory was used earlier by the authors of [4], who on the basis of observational data on three satellites for the first time obtained confirmation of the dependence of front position on the dynamic pressure of the solar wind.

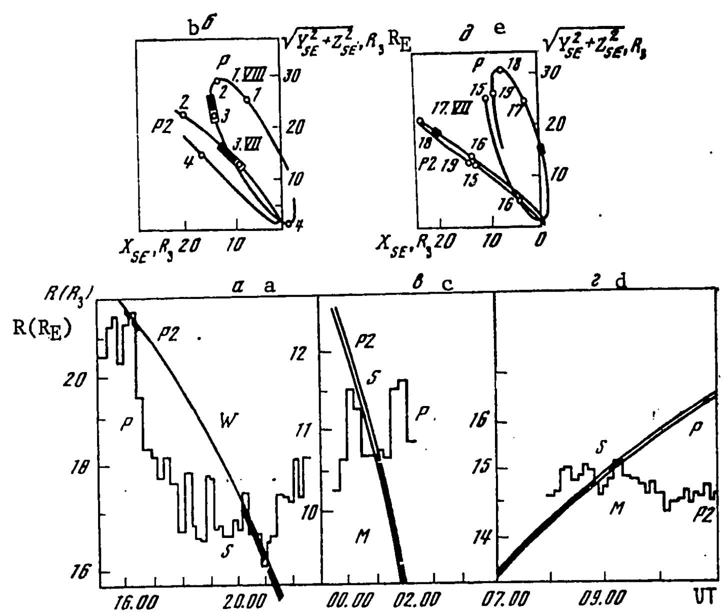

Fig. 1. Comparison of intersections of shock wave front and magnetopause observed on one of the "Prognoz" stations in July 1972 with the positions of these boundaries (stepped curve), computed on the basis of averaged data on the dynamic pressure of the solar wind obtained on the other station (a, c and d). The diagram shows the relative position of the "Prognoz" (P) and the "Prognoz-2" (P_2). Also given are the values of the φ angles (sun-earth-vehicle) at the times of the intersections. a) 2 July, φ= 57°, c) 3 July, d) 16 July, φ = 90-95°.

Figure 4 in solar-ecliptic coordinates (the X_{SE} axis passes through the center of the earth and is directed toward the sun) shows the positions of the "Prognoz" and "Prognoz-2" stations at the times of their intersections of the shock wave front (Fig. 4,a) and the magnetopause (Fig. 4,b): the dots correspond to single intersections of the boundaries, the segments of the dashed lines correspond to repeated intersections, the solid segments of the straight lines in Fig. 4,b show an indistinct transition from the transition region into the magnetosphere (see Section 2). The boundaries

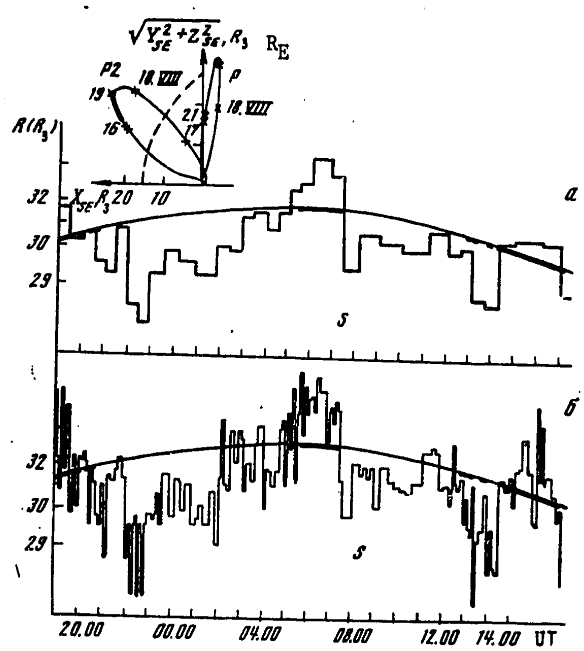

Fig. 2. Comparison of positions of shock wave front observed on the "Prognoz" station and positions of front computed on the basis of averaged (a) and unaveraged (b) data on the dynamic pressure of the solar wind obtained on the "Prognoz-2" station on 19 August 1972 (φ -- 98°).

were approximated by arbitrary second-order axially symmetric (relative to the X_{SE} axis) curves. The mean square distances along the normal to the boundary for the intersections shown in Fig. 4 were minimized for three parameters.

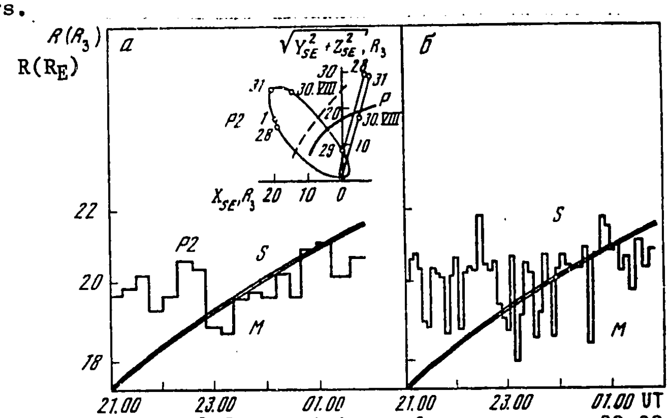

Fig. 3. Same as in Fig. 2 for positions of magnetopause 29-30 August 1972 (φ - 105°)

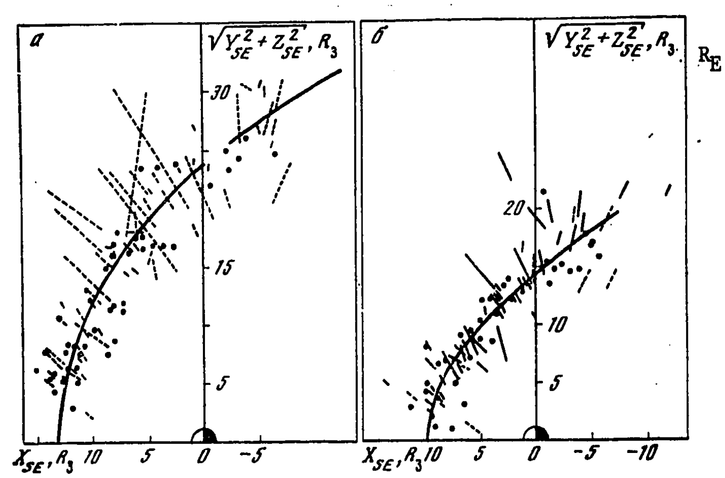

Fig. 4. Mean positions of shock wave front (a) and magnetopause (b), obtained using data on intersections of these boundaries at both stations during period April-October 1972.

Table 1 gives parameters characterizing the mean position of the front and magnetopause, computed in the approximation mentioned above.

It should be noted that in [5], on the basis of data from electrostatic analyzers aboard the "Prognoz" station, the mean position of the front was computed. The difference in the parameters of the mean front obtained in

[5] (hyperbola with ε = 1.09, p = 28.6 R_E, R_S = 13.7 R_E) from those obtained in this study can be related both to the use in [5] of a lesser amount of experimental points and to the fact that in that study there was minimizing of the mean square radial deviations of these points from a second-order axially symmetric curve with its focus at the center of the earth.

Table 1

Characteristics of Front and Magnetopause

Вид границы 1	Эксцентриситет ε 2	Лобовое расстояние $R_{S,M}$, $R_З$ 3	Параметр кривой p, $R_З$ 4	Положение фокуса X_F, $R_З$ 5
6 Фронт	0,85	13,1	23,4	0,5
7 Магнитопауза	1	9,9	10,1	4,5

KEY:

1. Type of boundary
2. Eccentricity ε
3. Frontal distance $R_{S,M}$, R_E
4. Parameter of curve p, R_E
5. Position of focus X_F, R_E
6. Front
7. Magnetopause

In Figures 1-3 the blackened segments of the orbits correspond to the time of presence of the stations in the transition region S and in the magnetosphere M, the thinned-unblackened segments represent the presence of the stations in the solar wind W and in the transition region S. In these figures the trajectories of the stations have been reduced to some fixed angles φ (see above); the distances scale (along the y-axis) is logarithmic, which made it possible to compare the computed graph - 1/6 lg (ρV^2) (stepped curve) with the observed intersections of the front and magnetopause by means of shifting of this curve parallel to the y-axis. Thereby it was possible to avoid use of an inexact empirical coefficient $C_{S,M}$ in formula (1) and a constant factor in computing ρV^2 from the measured spectra. We note that in computing the dynamic pressure of the solar wind the greatest contribution is made by the energy intervals with maximum readings (one-two intervals in the spectrum). Therefore, the computed values ρV^2 actually are the mean values for the time period $\lesssim$ 1-1.5 min.

The computed positions of the front and magnetopause in Figures 1, 2,a and 3,a were determined using the values of the dynamic pressure of the solar wind ρV^2, averaged for two-three spectra, that is (taking into account what has been said above) for 5-10 minutes, whereas in Fig. 2,b and Fig. 3,b -- on the basis of the ρV^2 values for each spectrum ($\lesssim$ 1-1.5 min).

Figures 1, 2,a and 3,a show that there is a rather good correspondence between the positions of the computed and observed limits. A comparison of these figures with Fig. 2,b and 3,b shows that the correspondence worsens considerably for unaveraged data. It can therefore be concluded that the characteristic time for the setting-in of quasistationary positions both of the shock wave front and the magnetopause with changes in pressure of the solar wind is ~5-10 min. We note that this time in order of magnitude agrees with the time of propagation of fast magnetosonic waves (~ 70-100 km/sec), transmitting "information" from the shock wave front to the magnetopause and back (at a distance $\Delta \sim 3-5\ R_E$).

A statistical investigation of the dependence of the positions of the front and magnetopause on the dynamic pressure of the solar wind, carried out using a great volume of data obtained using the one satellite IMP-4, was presented in [6]. The author concluded that the position of the magnetopause could be predicted more poorly than the position of the front. Evidently, this was associated with the great time gap between the moments when the satellite intersected the magnetopause and the period of its presence in the undisturbed solar wind, for which the dynamic pressure was determined.

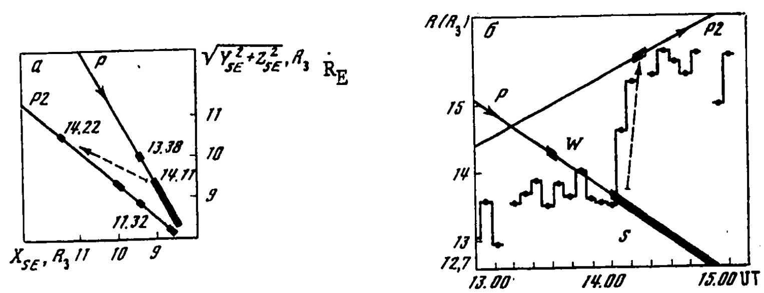

Fig. 5. Diagram determining the velocity of motion of the shock wave front using data from simultaneous observations on two stations on 3 July 1972. The notations are the same as in Fig. 1.

Simultaneous measurements on two spatially separated space vehicles can be used conveniently for a direct estimate of the velocity of motion of the shock wave front. Figure 5 shows a case when the "Prognoz" and "Prognoz-2" stations, flying toward one another, in the orbital segments situated in the subsolar region of circumterrestrial space, registered multiple intersection of the shock wave front. At 1411 UT the "Prognoz" intersected the shock wave front and entered the transition layer. At this time the "Prognoz-2," being situated in the solar wind, began to register a monotonic decrease in ρV^2, that is, the shock wave front must smoothly withdraw from the earth (without performing to-and-fro motions (Fig. 5,b). In actuality, at 1422 UT the front overtook the "Prognoz-2," also withdrawing from the earth. Thus, in 10 minutes the shock wave front passed $\sim 2R_E$ along the normal to its mean surface and its mean velocity, accordingly, was ~20 km/sec.

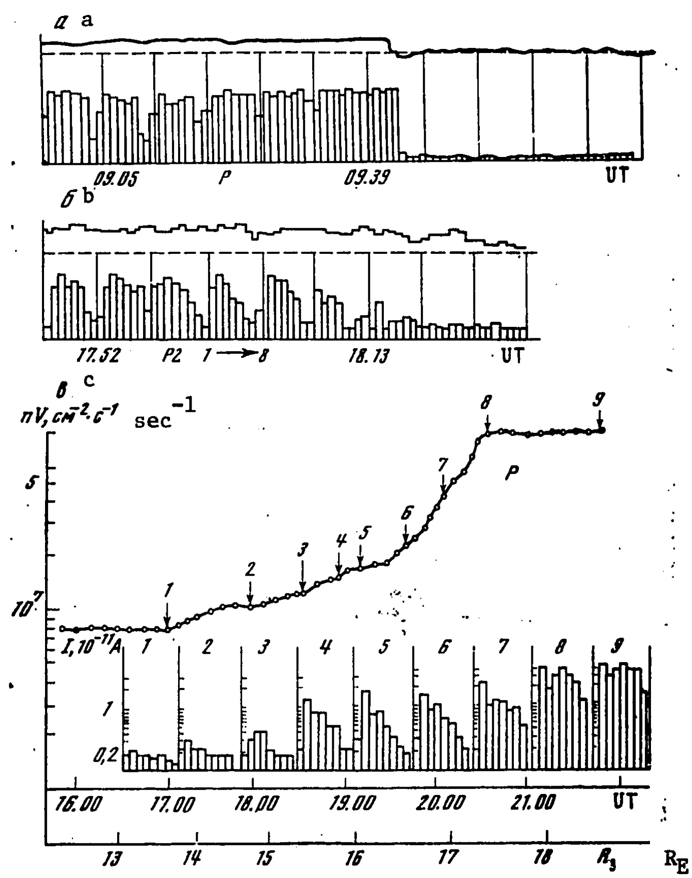

Fig. 6. Characteristic changes in form of ion spectra of modulation traps (upper curves in a and b -- currents of integral trap) during intersections: distinct magnetopause 28 May 1972 when φ - 6° and K_p - 3 (a) and diffuse magnetopause on 9 September 1972 when φ - 30°, K_p - 0, φ_{GSM} = 49°, λ_{GSM} = -56° (b) and 16 May 1972 when φ - 73°, K_p - 1, φ_{GSM} = 25°, λ_{GSM} = -1° (c). The change for the ion flux pV during intersection of the diffuse boundary on 16 May 1972 (c) is shown by the curve. The arrows with the figures denote the times UT which correspond to the spectra cited under the curves: 1) 1700, 2) 1800; 3) 1835; 4) 1900, 5) 1911, 6) 1938, 7) 2006, 8) 2038, 9) 2155

In another similar analyzed case (31 July 1972) the velocity of movement of the front was ~10 km/sec. These estimates in order of magnitude agree with the earlier obtained experimental estimates of the mean velocity of motion of the front $\sim$10-20 km/sec [7-9] and with theoretical computations [10, 11].

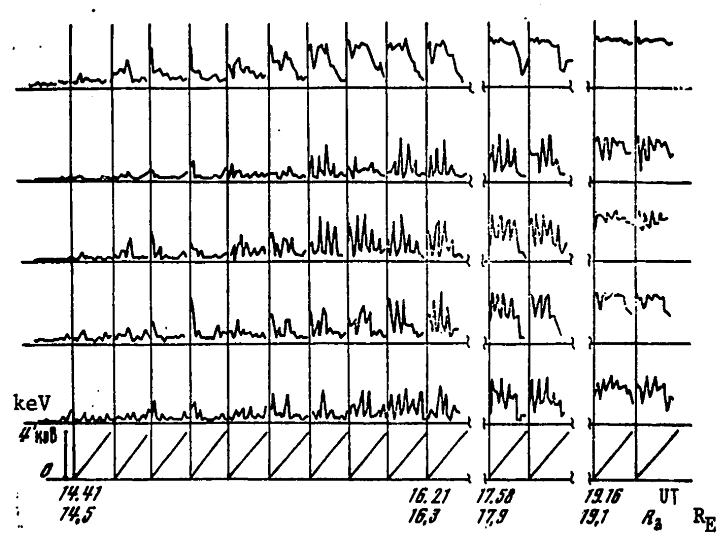

Fig. 7. Primary ion spectra obtained using five identical modulation ion traps on the "Prognoz-3" station on 8 April 1973 (φ_{SE} = 88°, λ_{SE} = 110°, φ = 90°) during intersection of diffuse magnetopause.

In [12], in which the velocity of motion of the front was computed using the Rankine-Hugoniot relationships, a mean velocity value $\sim$85 km/sec was obtained. Such evaluations involve considerable difficulties in determining the concentration and vector of the transport velocity of ions in the transition region, for which it is difficult to select a suitable form of the distribution function (for example, see [13]).

Evidently, one can agree with the authors of [10] in that the high velocities of movement of the front, obtained in some studies [12, 14], can be related to extremal conditions in the solar wind (exceedingly small values of the Mach number, tangential discontinuities with concentration jumps > 4 or $< 1/3$, by shock waves, etc.), which are realized rather rarely.

2. Investigation of Plasma Structure of Magnetopause

An analysis of intersections of the magnetopause by the "Prognoz" and "Prognoz-2" stations indicated that in 49 of the 93 considered cases there was a gradual change in the nature of the spectra, lasting from 10 minutes (in several cases) to several hours. With respect to such intersections the magnetopause will henceforth be called diffuse, as, for example, in [15, 16].

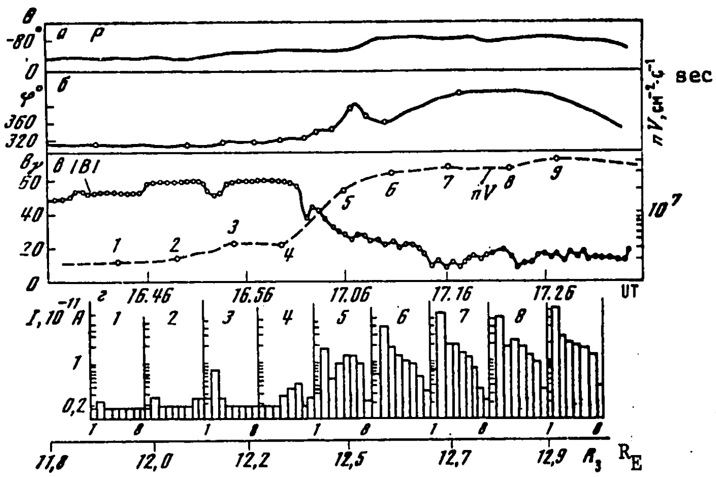

Fig. 8. Comparison of data from simultaneous measurements of the characteristics of ions and the magnetic field on the "Prognoz" station on 8 May 1972 with intersection of the diffuse magnetopause (φ_{SE} = 70°; λ_{SE} = -41°).

Table 2

Latitudinal Distribution of Number of Cases of Observation of Diffuse and Distinct Magnetopause

$\varphi_{экл}$, град 1	Магнитопауза 2		Всего 5	%
	диффузная 3	резкая 4		
0—30	24	23	47	51
30—50	8	14	22	36
50—70	17	7	24	71

KEY:

1. φ_{ecl}, degrees
2. Magnetopause
3. Diffuse
4. Distinct
5. Total

Figure 6,a shows an example of the characteristic change in the primary ion spectra and currents in the integral trap oriented on the sun during intersection of a distinct magnetopause on 28 May 1972 and Fig. 6,b is the same during intersection of the diffuse magnetopause on 9 September 1972. In the first case a marked change in the nature of the spectrum of the modulation trap and the current of the integral trap occurred in a time less than 40.8 sec. Figure 6,c illustrates the passage of the "Prognoz" station through the diffuse magnetopause on 16 May 1972; it shows changes in the ion flux

$$nV = 3.67 \cdot 10^{17} \sum_{i=1}^{\infty} I_i$$

(where I_i is the current in amperes registered in the i-th energy interval) and a number of spectra corresponding to the times noted on the nV curve by arrows with the figures 1, 2,..., etc.; also given are the angles φ (sun-earth-station) and K_p are indices relating to the period when the stations intersect the magnetopause. Figure 6,b,c shows that with transition from the transition region into the magnetosphere there is a smooth change (decrease) in the ion flux and a gradual softening of the spectra (relative decrease in the currents in the energy intervals corresponding to high energies) at the distance $\sim 2R_E$. The maximum gradient of the ion flux was observed at a distance $\sim 1R_E$.

A proof that the observed softening of the spectra is not a result of averting of the plasma flow from the trap during movement of the station into the magnetosphere are the results of measurements of ion spectra using five similar modulation traps on the "Prognoz-3" station in 1973 (Fig. 7). The axes of four of these traps formed an angle of 30° with the axis of the central trap, oriented on the sun; the ion spectrum in the energy range 0-4 keV was registered in 10 minutes in 16 energy intervals.

With diversion of the ion flux from the central trap by the angle α there will be modulation of the currents in the lateral traps due to rotation of the station about the axis of the central trap; when $\alpha > 15°$ the maximum flux will enter into one of the lateral traps. Figure 7 shows the currents in all five traps: the upper graph shows the currents in the central trap, whereas the lower graph shows the direction of the energy increase in each spectrum. Figure 7 shows that with intersection of the diffuse magnetopause in all the energy intervals the fluxes in the central trap exceed the maximum flux in the others, that is, the deviation of the direction of the ion flux from the direction of the axis of the central trap is an angle $< 15°$.

Figure 8 shows data from simultaneous measurements of the polar angle θ (Fig. 8,a), the azimuthal angle φ (Fig. 8,b), the absolute value $|B|$ (Fig. 8,c) of the magnetic field vector during intersection of the diffuse magnetopause; also shown are changes in the ion flux (dashed line in Fig. 8, c) and individual spectra (Fig. 8,d) corresponding to the times noted by the figures 1-9 on curve nV. The data from magnetic measurements were furnished through the courtesy of Sh. Sh. Dolginov and Ye. G. Yeroshenko. Figure 8 shows that with a smooth change in the spectra and the ion flux at a distance $\sim 0.5R_E$ during intersection of the diffuse magnetopause all the magnetic field characteristics also were free of marked jumps.

It can be seen from Fig. 4,b, in which segments of straight lines show the positions of the station during intersections of the diffuse magnetopause, that it was frequently observed with quite small φ angles and that its thickness on the average increases with an increase in φ.

Table 2 shows the numbers of cases of registry of diffuse and distinct magnetopauses, the total number of intersections of the magnetopause and the percentage number of observations of the diffuse magnetopause in the indicated intervals of solar-ecliptic latitudes.

Table 2 shows that most frequently the diffuse boundary was observed in the latitude zone 50-70° and 0-30°. However, it is necessary to deal with caution with the noted tendency in the latitudinal distribution of the diffuse magnetosphere due to the relatively small volume of data.

Comparison of observations of the diffuse boundary with data from simultaneous measurements of the interplanetary magnetic field on the "Geos-2" satellite [17] indicated that in the presence of a northerly component B_N of the interplanetary magnetic field the mean thickness of the diffuse magnetopause was $\sim 0.8R_E$, and in the presence of a southerly component B_S it increased to $\sim 2R_E$.

It can be concluded from a review of data in the literature that at the present time ideas have been developed concerning the magnetopause, at least in the subsolar region, as a distinct boundary (tangential or rotational discontinuity) with a thickness of the order of the Larmor radius of ions ~ 100 km (for example, see [7, 8, 16, 18, 19]. A diffuse boundary was observed in the tail of the magnetosphere on the vehicles "Pioneer-8" (at distances ~ 30-$40R_E$) [15], "Explorer-35" (near the lunar orbit $\sim 60R_E$) [20], and also on the "Vela" satellites (at a distance $\sim 18R_E$) [21, 22]. The authors note the absence of observations of a distinct boundary (diffuse magnetopause) on the basis of magnetic data on the vehicle IMP-1 [23, 24], OGO-1 (near the equatorial plane in the morning and evening sectors of the magnetosphere) [8], on the basis of plasma and magnetic data on the vehicle IMP-2 [16] in the subsolar region of the magnetosphere.

In laboratory experiments [25] there was an inflow of plasma into the regions of the polar cusps (the same as in experiments on space vehicles [26, 27]) and into the equatorial "slot," beginning on the daytime side of the artificial magnetosphere at approximately 1400 UT and passing into the tail of the magnetosphere. Finally, in a number of theoretical studies there is a discussion of the interaction between the plasma in the transition region and the magnetosphere (viscouslike interaction [28], rejoining of the lines of force of the interplanetary magnetic field, having a southerly component, with the terrestrial dipole field [29], development on the boundary of different plasma instabilities, for example [24, 30]), which can lead to a blurring of the distinct boundary of the magnetosphere.

As can be concluded from the characteristics of the diffuse magnetopause, observed on the "Prognoz" and "Prognoz-2" stations and described in this study, it resembles the boundary layer discovered in the tail of the magnetosphere on the "Vela" satellites [21, 22].

The latitudinal distribution of the diffuse boundary has a tendency similar to the observational data [8, 26, 27] and laboratory experiments [25], indicating a possible inflow of plasma into the polar and equatorial slots and an instability of the magnetopause at these latitudes. This similarity, and also some dependence of the thickness of the diffuse magnetopause, registered on the "Prognoz" and "Prognoz-2," on the presence of a southerly component of the interplanetary magnetic field, can be discussed in connection with the mechanisms of origin of the diffuse magnetopause and require further investigation.

BIBLIOGRAPHY

1. Bezrukikh, V. V., Belyashin, A. P., Volkov, G. I., et al., GEOMAGNETIZM I AERONOMIYA (Geomagnetism and Aeronomy), 14, No 3, 400, 1974.

2. Gringauz, K. I., Zastenker, G. N., Khokhlov, M. Z., KOSMICHESKIYE ISSLEDOVANIYA (Space Research), 12, No 6, 899, 1974.

3. Spretter, J. R., Summers, A. L., Alksne, A. Y., PLANET. SPACE SCI., 14, 223, 1966.

4. Binsack, J. H., Vasyliynas, V. M., JGR, 73, 429, 1968.

5. Vaysberg, O. L., Zertsalov, A. A., Temnyy, V. V., Berezin, Yu. Ye., KOSMICHESKIYE ISSLEDOVANIYA, 12, No 1, 80, 1974.

6. Fairfield, D. H., JGR, 76, 6700, 1971.

7. Holzer, R. E., McLeod, M. G., Smith, E. J., JGR, 7, 148, 1966.

8. Heppner, J. P., Sugiura, M., Skillman, T. L., et al., JGR, 72, 5417, 1967.

9. Kaufmann, R. L., JGR, 72, 2323, 1967.

10. Volk, H. J., Auer, R. D., JGR, 79, 40, 1974.

11. Auer, R. D., JGR, 79, 34, 5122, 1974.

12. Formisano, V., Hedgecock, P. C., Moreno, G., et al., JGR, 78, 3731, 1973.

13. Formisano, V., Moreno, G., Palmiotto, F., Hedgecock, P. C., JGR, 78, 19, 3714, 1973.

14. Grinstadt, E. W., Hedgecock, P. C., Russell, C. T., JGR, 77, 1116, 1972.

15. Intriligator, D. S., Wolf, J. H., JGR, 77, 5480, 1972.

16. Fairfield, D. H., Ness, N. F., JGR, 72, 2379, 1967.

17. Hedgecock, P. C., GEOS INTERPLANETARY FIELD MEASUREMENTS, S. Preprint, London, S. W. 7, Imper. College Phys. Dept., 1973.

18. Cahill, L. J., Patel, V. L. Jr., PLANET. SPACE SCI., 15, 997, 1967.

19. Aubry, M. P., Kivelson, M. G., Russell, C. T., JGR, 76, 1673, 1971.

20. Howe, C. H., Siscoe, G. L., JGR, 77, 6071, 1972.

21. Hones, E. W., Jr., Asbridge, J. R., Bame, S. J., et al., JGR, 77, 5503, 1972.

22. Akasofu, S. I., Hones, E. W., Jr., Bame, S. J., et al., JGR, 78, 7257, 1973.

23. Ness, N. F., Scearce, C. S., Seak, J. B., JGR, 69, 3531, 1964.

24. Boller, B. R., Stolov, H. L., JGR, 78, 8078, 1973.

25. Dubinin, E. M., Podgorny, L. M., JGR, 79, 1926, 1974.

26. Frank, L. A., JGR, 76, 5202, 1971.

27. Russell, C. T., Chappel, C. R., Montgomery, M. D., et al., JGR, 76, 6743, 1971.

28. Axford, W. I., PLANET. SPACE SCI., 12, 45, 1964.

29. Dungey, J. M., PHYS. REV. LETTERS, 6, 47, 1961.

30. Southwood, D. J., PLANET. SPACE SCI., 16, 587, 1968.

[8144/1843-5303]

5303
CSO: 8144 / 1843

UDC 629.7.014.18

CONTROL SYSTEMS OF SPACE VEHICLES STABILIZED BY ROTATION

Moscow SISTEMY UPRAVLENIYA KOSMICHESKIKH APPARATOV, STABILIZIROVANNYKH VRASHCHENIYEM (Control Systems of Space Vehicles Stabilized by Rotation) in Russian 1979 pp 2, 293-295

[Annotation and table of contents from book by Yu. P. Artyukhin, L. I. Kargu and V. L. Simayev, Izdatel'stvo Nauka, 295 pages]

[Text] This book is devoted to the problem of the active control of rotating space vehicles (KA). It examines the questions of the dynamics of KA movement stabilized by rotation (transitional regiments, types of oscillation exhibited, possible angular changes around the axis, etc.).

The principles for developing a control system of the speed of rotation and the orientation of the rotating KA are presented. Linear and non-linear control systems are examined according to general features, the principles of control and the structural schemes of systems, the methods of calculating energy expenditures for supporting the given rotation speed. Materials are presented on the simultaneous utilization of final control elements (reactive and magnetic systems) for controlling the orientation as well as the speed of rotation of the KA. An algorithm designed for a computer magnetic control system is developed. The possibilities for the use of rotating KA's and the basic features of the means for securing vital activity and work capability in astronauts are examined.

This book is intended for specialists in space technology, mechanics, and the automatic control and applied theory of gyroscopes as well as for students of upper division courses in higher technical institutions.

Contents Page

[8144/1834-8228]

8228 -END-
CSO: 8144 / 1834